NJC

Accepted Manuscript

This article can be cited before page numbers have been issued, to do this please use: S. Roy, S. Chattopadhyay, M. G. B. Drew, A. Bauza and A. Frontera, *New J. Chem.*, 2018, DOI: 10.1039/C7NJ05148D.

View Article Online
DOI: 10.1039/C7NJ05148D

Non-covalent tetrel bonding interactions in hemidirectional lead(II) complexes with nickel(II)-salen type metalloligands

Sourav Roy,[a] Michael G. B. Drew,[b] Antonio Bauzá,[c] Antonio Frontera[c] and Shouvik Chattopadhyay*[a]

[a]Department of Chemistry, Inorganic Section, Jadavpur University, Kolkata - 700032, India. Tel: +9133-2457-2941; E-mail: shouvik.chem@gmail.com

[b]School of Chemistry, The University of Reading, P.O. Box 224, Whiteknights, Reading RG6 6AD, United Kingdom,

[c]Department of Chemistry, Universitat de les Illes Balears, Crta de Valldemossa km 7.5, 07122 Palma de Mallorca (Baleares), SPAIN; E-mail: toni.frontera@uib.es

Abstract: Four hetero-dinuclear nickel(II)/lead(II) complexes have been synthesized and characterized. Structures have been confirmed by single crystal X-ray diffraction studies. In each complex, nickel(II) is placed in the inner N_2O_2 compartment and lead(II) in the outer O_2O_2' compartment of the respective Schiff base. In complexes **1**, **3** and **4,** lead(II) centres are hemidirectionally coordinated, and thus are well suited for establishing tetrel bonding interactions which have been investigated thoroughly by means of DFT calculations.

Keywords: Lead(II); Nickel(II); Heteronuclear; Compartmental Schiff base, Tetrel bonding, Supramolecular interactions.

View Article Online
DOI: 10.1039/C7NJ05148D

Introduction

Although lead is a deadly toxic element and is a dangerous biological poison similar to mercury[1], its large radius, adoption of different coordination numbers or valences etc leading to versatile coordination chemistry attracted synthetic inorganic chemists to prepare new lead(II) complexes.[2] Despite the negative functions associated with lead(II) related to pollution and health, lead containing materials are increasingly used in batteries, non-linear optical materials, ferroelectric materials and semiconductors.[3] $Na_2CaEDTA$ is a well-known drug used to trap lead(II) from human body[4], and it is a very challenging task currently to develop other chelating ligands for the treatment of lead intoxication.[5] In the present work, salen type $N_2O_2O'_2$ donor compartmental Schiff bases have been used to trap nickel(II) in the inner N_2O_2 cores and these nickel(II)-salen type metalloligands have been, in turn, used to lock lead(II) in outer $O_2O'_2$ cores. Salen type ligands are very common in literature due to their ease in synthesis and tendency to ligate a variety of transition metal ions in tetradentate N_2O_2 cores.[6,7] 1,3-propane diamine is used to prepare these salen type ligands because of the enhanced stability of six member unsaturated chelate ring (Ni-N-C-C-C-N-Ni). These heteronuclear complexes may have potential applications in gas separation and encapsulation[8], hydrometallurgy[9], metal clusters[10], material science[11], transport and activation of small molecules[12] etc. The valence shell electronic configuration of lead is $4f^{14}5d^{10}6s^26p^2$. The $6s^2$ electron pair remains as inert primarily as a result of increasing effective nuclear charge due the presence of imperfectly screening f^{14} and d^{10} electrons. High penetrating property of the 6s orbital and relativistic stabilization of $6s^2$ electrons are also major reasons for lead to show the inert pair effect.[13] The extent to which the

View Article Online
DOI: 10.1039/C7NJ05148D

lone pair is stereochemically active[14] is currently proving an interesting research topic for the theoretical chemists.[15]

In addition to the widely used hydrogen bonding interactions for the construction of metal organic frameworks (MOFs), other directional interactions such as σ-hole interactions are becoming interesting players.[16,17] It is well-known that the size and electron deficiency of σ–holes increase with the polarizability of the Lewis acid atom. Strong σ–hole interactions occur in complexes where a heavy atom of groups IV to VII is covalently bonded to electronegative ones. These interactions have been widely described for chalcogen, pnictogen and halogen atoms. However, those of group IV involving tetrel bonding interactions are scarcely to be found in the literature,[18] in spite of the fact that it has been shown that they can be markedly strong (especially in the cases of tin and lead). For instance, the design and synthesis of lead(II) MOFs based on covalent and non-covalent tetrel bonding have been reported.[19,20] In these MOFs, Pb···S and Pb···N non-covalent tetrel bonds interconnect the covalently bonded units into supramolecular assemblies. It has been also shown that tetrel bonds with hemi-directionally coordinated lead(II) occur with high probability and predictable geometries, thus playing an important role in the solid-state chemistry of lead. As a matter of fact, the divalent form of lead Pb(II), presents a special interest for physical chemists due to its unusual coordination properties, which are highly versatile and flexible. It is characterized by a large variety of coordination numbers and a structural organisation in two distinct classes (Scheme 1). One is named holodirected structure, in which the bonds to ligand atoms are directed throughout the surface of an encompassing sphere. The other is named hemidirected structure, in which the bonds to ligand atoms are directed throughout a hemisphere and thus exhibit a clear void in

View Article Online
DOI: 10.1039/C7NJ05148D

the distribution of bonds to the ligands.[21a] It has been shown that Pb(II) complexes with a variety of ligands are hemidirected for coordination number up to five (n ≤ 5), and holodirected for coordination number six and higher (n ≥ 6).[21]

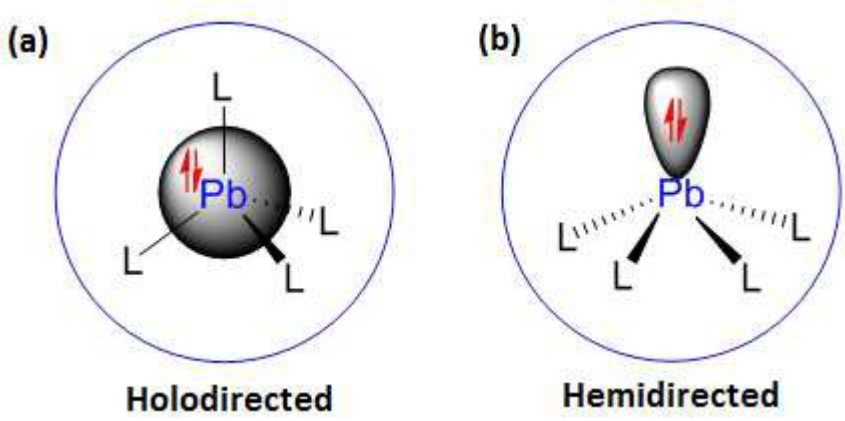

Scheme 1: Schematic representation of the holodirected (a) and hemidirected (b) coordination modes of lead(II), with indication of the location of the inert lone pair.

In the present work, we used three compartmental Schiff bases, H_2L^1 [N,N'-bis(3-methoxysalicylidene)-2,2-dimethylpropane-1,3-diamine], H_2L^2 [N,N'-bis(3-ethoxysalicylidene)propane-1,3-diamine] and H_2L^3 [N,N'-bis(3-ethoxysalicylidene)-2,2-dimethylpropane-1,3-diamine], to prepare four heterodinuclear nickel(II)/lead(II) complexes, *$[(H_2O)Ni(SCN)L^1Pb(OAc)]\cdot DMSO$* (**1**), *$[(H_2O)_2NiL^2PbCl_2]$* (**2**), *$[(SCN)NiL^2(OAc)Pb]$* (**3**), *$[(H_2O)Ni(SCN)L^3PbCl]$* (**4**). Their structures have been determined by single crystal X-ray diffraction analyses. Interestingly, in three complexes (**1, 3** and **4**) the lead(II) is hemi-directionally coordinated (n = 5) and in two of them (**1** and **3**) the lead(II) participates in non-covalent tetrel bonding interactions. These forces along with other non-covalent interactions control the supramolecular architectures and organometallic frameworks observed in their solid state architecture. The lead(II) presents a coordination mode in which it has a clear void in

View Article Online
DOI: 10.1039/C7NJ05148D

the distribution of bonds to the ligands as usual in hemi-directional coordination.[21] Such a void facilitates the approach of electron donors to the lead(II) enabling the formation of a strong tetrel bond with a predictable geometry. The nature of the tetrel bonds in both structures (**1** and **3**) was studied by DFT calculations, which showed the presence of the σ-hole at the lead(II) and the considerable strength of these interactions.

Experimental Section

Nickel(II) thiocyanate tetrahydrate was prepared in the laboratory following the literature method.[22] All other materials were commercially available, reagent grade and used as purchased from Sigma-Aldrich without further purification.

Synthesis

Synthesis of ligands

Synthesis of H_2L^1 [N,N'-bis(3-methoxysalicylidene)-2,2-dimethylpropane-1,3-diamine]

A methanol solution (10 mL) of 3-methoxysalicylaldehyde (300 mg, 2 mmol) and 1,3-diaminopropane (0.13 mL, 1 mmol) was refluxed for ca. 1 h to prepare H_2L^1. The ligand was not isolated and used directly for the synthesis of complex **1**.

Synthesis of H_2L^2 [N,N'-bis(3-ethoxysalicylidene)propane-1,3-diamine] and H_2L^3 [N,N'-bis(3-ethoxysalicylidene)-2,2-dimethylpropane-1,3-diamine]

Similarly, methanol solution (10 mL) of 3-ethoxysalicylaldehyde (332 mg, 2 mmol) was refluxed with 1,3-diaminopropane (0.13 mL, 1 mmol) and 2,2-dimethyl-1,3-diaminopropane

View Article Online
DOI: 10.1039/C7NJ05148D

(0.12 mL, 1 mmol) separately, for ca. 1 h to prepare H_2L^2 and H_2L^3 respectively. The ligands were not isolated and used directly for the synthesis of complexes **2**-**3** (H_2L^2) and **4** (H_2L^3).

Synthesis of complexes

*Synthesis of [$(H_2O)Ni(SCN)L^1Pb(OAc)$]·DMSO (**1**)*

A methanol (10 mL) solution of lead(II) acetate trihydrate (380 mg, 1 mmol) was added to the methanol solution (20 mL) of H_2L^1 and the resulting solution was stirred for 15 min. A methanol (10 mL) solution of nickel(II) thiocyanate tetrahydrate (250 mg, 1 mmol) was then added to it. Stirring was continued for about 2h. A few drops of DMSO were then added to the solution. Single crystals, suitable for X-ray diffraction, were obtained after 3-4 days on slow evaporation of the solution in open atmosphere.

Yield: 557 mg (68%). Anal. Calc. for $C_{24}H_{31}N_3NiO_8PbS_2$ (FW = 819.55): C, 36.47; H, 3.86; N, 5.55; Found: C, 36.3; H, 3.7; N, 5.6%. FT-IR (KBr, cm^{-1}): 1632 (C=N); 2070 (NCS); 1470, 1419 (C=O). UV-VIS [λ_{max}(nm)] [ε_{max}($Lmol^{-1}cm^{-1}$)] (DMF): 268 (1.8×10^4); 293 (3.3×10^3); 363 (3.1×10^3); 581 (12.2); 813 (15.1).

*Synthesis of [$(H_2O)_2NiL^2PbCl_2$] (**2**)*

A methanol (10 mL) solution of lead(II) nitrate (332 mg, 1 mmol) was added to the methanol solution (20 mL) of H_2L^2 and the resulting solution was stirred for 15 min. A methanol (10 mL) solution of nickel(II) chloride hexahydrate (237 mg, 1 mmol) was then added to it. Stirring was continued for about 2h. Single crystals, suitable for X-ray diffraction, were obtained after 3-4 days on slow evaporation of the solution in open atmosphere.

View Article Online
DOI: 10.1039/C7NJ05148D

Yield: 496 mg (67%). Anal. Calc. for $C_{21}H_{28}Cl_2N_2NiO_6Pb$ (FW = 741.24): C, 34.05; H, 3.83; N, 3.80; Found: C, 33.9; H, 3.7; N, 3.9%. FT-IR (KBr, cm^{-1}): 1624 (C=N). UV-VIS [λ_{max}(nm)] [ε_{max}($Lmol^{-1}cm^{-1}$)] (Acetonitrile): 231 (2.2×10^4); 269 (1.04×10^4); 348 (3.6×10^3); 568 (9.11); 814 (29.8)

*Synthesis of [(SCN)NiL^2(OAc)Pb] (**3**)*

A methanol (10 mL) solution of lead(II) acetate trihydrate (380 mg, 1 mmol) was added to the methanol solution (20 mL) of H_2L^2 and the resulting solution was stirred for 15 min. A methanol (10 mL) solution of nickel(II) thiocyanate tetrahydrate (250 mg, 1 mmol) was then added to it. Stirring was continued for about 2h. Single crystals, suitable for X-ray diffraction, were obtained after 3-4 days on slow evaporation of the solution in open atmosphere.

Yield: 526 mg (70%). Anal. Calc. for $C_{24}H_{27}N_3NiO_6PbS$ (FW = 751.44): C, 38.36; H, 3.62; N, 5.59; Found: C, 38.2; H, 3.5; N, 5.7%. FT-IR (KBr, cm^{-1}): 1631 (C=N); 2101 (NCS); 1456, 1228 (N=O). UV-VIS [λ_{max}(nm)] [ε_{max}($Lmol^{-1}cm^{-1}$)] (DMF): 265 (4.4×10^3); 285 (1.9×10^3); 354 (1.8×10^3); 585 (3.5); 877 (5.2).

*Synthesis of [(H_2O)Ni(SCN)L^3PbCl] (**4**)*

A methanol (10 mL) solution of lead(II) nitrate (332 mg, 1 mmol) was added to the methanol solution (20 mL) of H_2L^3 and the resulting solution was stirred for 15 min. A methanol (10 mL) solution of nickel(II) chloride hexahydrate (237 mg, 1 mmol) was then added to it. After 15 min of stirring, methanol (10 mL) solution of sodium thiocyanate (81 mg, 1 mmol) was added

View Article Online
DOI: 10.1039/C7NJ05148D

to it. Stirring was continued for about 2h. Single crystals, suitable for X-ray diffraction, were obtained after 3-4 days on slow evaporation of the solution in open atmosphere.

Yield: 503 mg (65%). Anal. Calc. for $C_{24}H_{30}ClN_3NiO_5PbS$ (FW =773.92): C, 37.25; H, 3.91; N, 5.43; Found: C, 37.1; H, 3.7; N, 5.5%. FT-IR (KBr, cm^{-1}): 1633 (C=N); 2098 (C≡N). UV-VIS [λ_{max}(nm)] [ε_{max}($Lmol^{-1}cm^{-1}$)] (Acetonitrile): 232 (3.4×10^4); 270 (2.1×10^4); 348 (8.1×10^3); 548 (34.9); 833 (14.4).

Physical measurements

Elemental analyses (carbon, hydrogen and nitrogen) were performed using a Perkin Elmer 240C elemental analyzer. IR spectra in KBr (4500-500 cm^{-1}) were recorded with a Perkin Elmer Spectrum Two spectrophotometer. Electronic spectra in acetonitrile (for complexes **2** and **4**) and DMF (for complexes **1** and **3**) were recorded on a Perkin Elmer Lambda 35 UV-visible spectrophotometer. Steady state photoluminescence spectra in acetonitrile (for complexes **2** and **4**) and DMF (for complexes **1** and **3**) were obtained in Shimadzu RF-5301PC spectrofluorometer at room temperature. Time dependent photoluminescence spectra were recorded using Hamamatsu MCP photomultiplier (R3809) and were analyzed by using IBHDAS6 software. Emissions of complexes are tentatively attributed to the intra-ligand transitions modified by metal coordination. Intensity decay profiles were fitted to the sum of exponentials series $I(t)=\sum_i \alpha_i \exp\left(-t/\tau_i\right)$, where α_i was a factor representing the fractional contribution to the time resolved decay of the component with a lifetime of τ_i. Bi-exponential function was used to fit the decay profile for complexes, with obtaining χ^2 close to 1. The intensity-averaged

View Article Online
DOI: 10.1039/C7NJ05148D

life times (τ_{av}) were determined from the result of the exponential model using $\tau_{av} = \frac{\sum_i \alpha_i \tau_i^2}{\sum_i \alpha_i \tau_i}$,

where α_i and τ_i are the pre-exponential factors and excited state luminescence decay time associated with the *i*-th component, respectively.

X-ray crystallography

Suitable crystals of complexes **1**-**4** were picked, mounted on a glass fiber and diffraction intensities were measured with an Oxford Diffraction XCalibur diffractometer equipped with Mo K_α radiation (λ =0.71073 Å, 50 kV, 40 mA) at 150 K. Data collection and reduction were performed with the Oxford diffraction Crysalis software.[23] The structures of the complexes were solved by direct methods using the SHELXS-97 program.[24] Non-hydrogen atoms were refined anisotropically. Hydrogen atoms attached to nitrogen and oxygen atoms were located by difference Fourier maps. The structures were refined on F^2 using SHELX2016-6.[24] Other programs used included PLATON,[25] DIAMOND,[26] ORTEP[27] and MERCURY.[28]

Hirshfeld surfaces

The Hirshfeld surface[29] of complexes **1**-**4** were determined using Crystal Explorer.[30]

Theoretical Methods

The geometries of the complexes included in this study were computed at the M06-2X/def2-TZVP level of theory using the crystallographic coordinates within the TURBOMOLE program.[31] This level of theory is adequate for studying non-covalent interactions in organometallic complexes. The basis set superposition error for the calculation of interaction

View Article Online
DOI: 10.1039/C7NJ05148D

energies has been corrected using the counterpoise method.[32] The "atoms-in-molecules" (AIM)[33] analysis of the electron density has been performed at the same level of theory using the AIMAll program.[34]

Results and Discussion

Synthesis

1,3-diaminopropane was refluxed separately, with 3-methoxysalicylaldehyde and 3-ethoxysalicylaldehyde, respectively, in 1:2 ratio to form two N_2O_4 donor compartmental Schiff base ligands, H_2L^1 and H_2L^2 respectively, following the literature method.[35] 3-ethoxysalicylaldehyde on refluxing with 2,2-dimethyl-1,3-diaminopropane in 2:1 ratio gave another N_2O_4 donor compartmental Schiff base ligand H_2L.[3,36] The Schiff base (H_2L^1) on reaction with lead(II) acetate trihydrate, followed by the addition of nickel(II) thiocyanate tetrahydrate and DMSO respectively gave heteronuclear complex **1**. Complex **2** was prepared by reacting Schiff base, H_2L^2, with lead(II) nitrate followed by the addition of nickel(II) chloride hexahydrate. Complex **3** was prepared by reacting Schiff base, H_2L^2 with lead(II) acetate trihydrate followed by the addition of nickel(II) thiocyanate tetrahydrate. Similarly, complex **4** was prepared by reacting Schiff base, H_2L^3 with lead(II) nitrate followed by the addition of nickel(II) chloride hexahydrate and sodium thiocyanate. Formation of all complexes is shown in Scheme 2.

The synthetic procedure has been repeated by adding nickel(II) first followed by the addition of lead(II). However, same complexes have been formed in all cases with nickel(II) occupying inner N_2O_2 and lead(II) occupying outer O_2O_2' cavities. This is probably because of the larger size of lead(II), the ionic radius of which (133 pm) is much larger compared to that of

View Article Online
DOI: 10.1039/C7NJ05148D

nickel(II) (83 pm). Therefore, it is difficult for lead(II) to be accommodated in compact (and therefore smaller) inner N_2O_2 compartment, where smaller nickel(II) fits well. Lead(II) on the other hand, fits well in the open (and therefore bigger) outer O_2O_2' compartment.

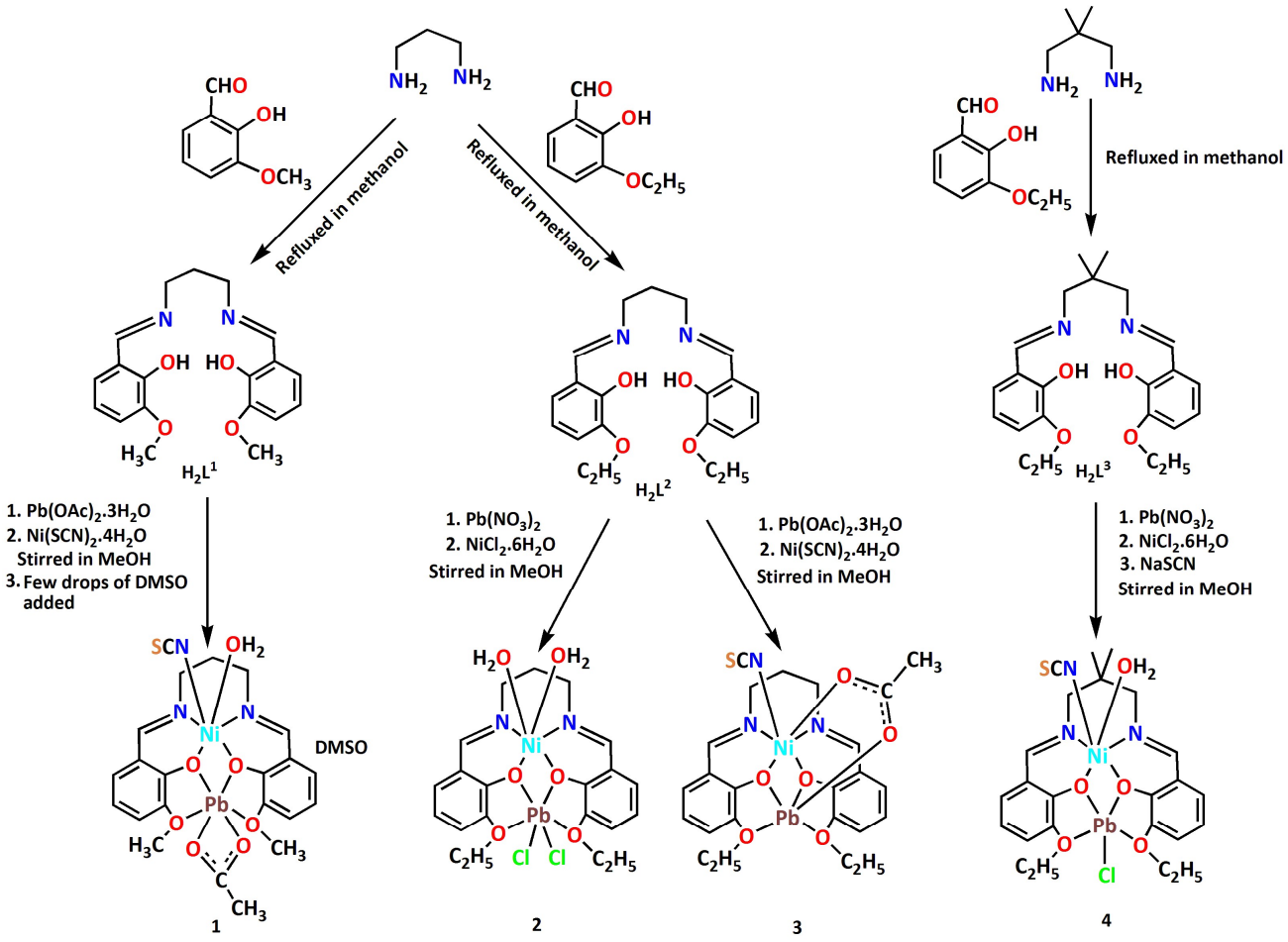

Scheme 2: Preparation of ligands and complexes.

Synthesis and X-ray characterization of several heteronuclear nickel(II)/lead(II) complexes could be found in literature (Table 1).[37] Tetrel bonding interactions have not been explored in any complex. Thus the present work is the first systematic study to explore tetrel bonding interactions in hemidirected heteronuclear nickel(II)/lead(II) complexes.

View Article Online
DOI: 10.1039/C7NJ05148D

Table. 1: Previously reported X-ray characterized heteronuclear nickel(II)/lead(II) complexes.

Complex (CCDC)	Formula	Coordination mode of lead	Tetrel Bonding	Pb-X (Å)	Ref
AYAKUG	$[Pb(OAc)(NiL^1)_2](OAc)$	Holodirected	Not explored	-	37a
UGENIF	$[NiL^2(H_2O)_2PbBr_2]$	Hemidirected	Not explored	-	37b
UGENOL	$[NiL^2(H_2O)_2Pb(NO_3)_2]$	Hemidirected	Not explored	-	37b
YISROI	$[\{L^3Ni\}Pb(NC_5H_5)Cl]_2$	Hemidirected	Not explored	3.423(6)	37c
YISRUO	$[\{L^4Ni\}_2Pb](H_2O)(Py)$	Hemidirected	Not explored	3.22(2)	37c
XUMGER	$\{[NiL^5(py)_2]PbCl_2\}(Py)$	Hemidirected	Not explored	3.006(4)	37d
ECEBAR	$[NiL^6Pb(NO_3)_2]$	Hemidirected	Not explored	2.976(7)	37e
PUYLEA	$[PbNiL^7(AcO)_2]$	Hemidirected	Not explored	-	37f
-	$[(H_2O)Ni(SCN)L^8Pb(OAc)]\cdot DMSO$	Hemidirected	present	3.379(4)	This Work
-	$[(H_2O)_2NiL^9PbCl_2]$	Hemidirected	absent	-	This Work
-	$[(SCN)NiL^9Pb(NO_3)]$	Hemidirected	present	3.064(2)	This Work

View Article Online
DOI: 10.1039/C7NJ05148D

-	$[(H_2O)Ni(SCN)L^{10}PbCl]$	Hemidirected	absent	- This Work

Where, H_2L^1 = N,N'-bis(3-methoxysalicylidene)ethane-1,2-diamine; H_2L^2 = N,N'-bis(3-ethoxysalicylidene)propane-1,3-diamine; L^3 = tris-((2-hydroxybenzylidene)-aminoethyl)amine; L^4 = tris-((-2-hydroxybenzylidene)-aminomethyl)propane; H_2L^5 = N,N'-bis(salicylidene)propane-1,3-diamine; H_2L^6 = N,N'-bis(3-ethoxysalicylidene)ethane-1,2-diamine; H_2L^7 = N,N'-dimethyl-N,N'-ethylene-di(5-bromo-3-formyl-2-hydroxybenzylamine); H_2L^8 = [N,N'-bis(3-methoxysalicylidene)-2,2-dimethylpropane-1,3-diamine], H_2L^9 = N,N'-bis(3-ethoxysalicylidene)propane-1,3-diamine; H_2L^{10} = N,N'-bis(3-ethoxysalicylidene)-2,2-dimethylpropane-1,3-diamine.

Structure description

The X-ray crystal structure determination reveals that both complexes **1** and **4** crystallize in triclinic space group $P\bar{1}$, whereas complexes **2** and **3** crystallize in monoclinic space group *C2/c* and $P2_1/n$ respectively. Details of crystallographic data and refinement details are given in Table 2. Important bond lengths and bond angles are gathered in Tables 3 and S1 {ESI (Electronic Supplementary Information)} respectively.

The molecular structures of complexes **1**-**4** are built from isolated hetero-dinuclear units of *$[(H_2O)(SCN)NiL^1Pb(OAc)]$* (Fig. 1)*, $[(H_2O)_2NiL^2PbCl_2]$* (Fig. 2)*, $[(SCN)NiL^2(OAc)Pb]$* (Fig. 3) *and $[(H_2O)(SCN)NiL^3PbCl]$* (Fig. 4) respectively. Only complex **1** contains a lattice DMSO molecule. Three $N_2O_2O_2'$ donor compartmental Schiff bases (H_2L^1-H_2L^3) are used to prepare the complexes

View Article Online
DOI: 10.1039/C7NJ05148D

in which nickel(II) centres are placed in inner N_2O_2 cavities and lead(II) centres are placed in outer O_2O_2' cavities. Nickel(II) centre in each complex is hexacoordinated and assumes distorted octahedral geometry. Lead(II) centres, are pentacoordinated, in complexes **1**, **3** and **4**. On the other hand, lead(II) centre is hexacoordinated in complex **2**. It is also to be noted that the central carbon atom, C21, of the propylene link in complex **2** is disordered off the two-fold axis in two possible positions (C21A and C21B).

The nickel(II) centre, [Ni(1)] has pseudo-octahedral geometry, where two imine nitrogen atoms, {N(19) and N(23) [for complexes **1**, **3** and **4**]; N(19) and N(19^i) {^{i} = symmetry transformation; -x, y, ½-z} [for complex **2**]} and two phenoxo oxygen atoms, {O(11) and O(31) [for complexes **1**, **3** and **4**]; O(11) and O(11^i) [for complex **2**]} of the deprotonated di-Schiff base constitute the equatorial plane. In case of complex **2**, N(19), N(19^i), O(11) and O(11^i) of the deprotonated di-Schiff base constitute the equatorial plane, which is almost planar with none of these atoms giving rise to r.m.s. deviation more than 0.042 Å. The nickel(II) is perforce on the two-fold axis in the equatorial plane. On the other hand, deviations of the coordinating atoms from the mean equatorial planes passing through them and that of the nickel(II) centres from the same planes in complexes **1**, **3** and **4** are listed in Table 4.

The axial positions of nickel(II) centres are occupied by nitrogen and/or oxygen atoms: one oxygen atom, O(1), from a water molecule and one nitrogen atom, N(1), from a thiocyanate molecule in complex **1**, two oxygen atoms, O(1) and O(1)^i [^{i} = symmetry transformation = -x, y, ½-z] in complex **2**, a nitrogen atom, N(1), from a thiocyanate and an oxygen atom, O(1), from an acetate in complex **3**, an oxygen atom, O(1), from a water molecule and a nitrogen atom, N(1), from a thiocyanate in complex **4**. All nickel(II)-nitrogen and nickel(II)-

View Article Online
DOI: 10.1039/C7NJ05148D

oxygen bond lengths are comparable to that observed in other complexes with similar structures.[38] Phenoxo oxygen atoms {O(11) and O(31) [for complexes **1**, **3** and **4**]; O(11) and O(11^{i}) [for complex **2**]} of deprotonated Schiff bases also coordinate to lead(II) centres. The potential donor ethoxy oxygen atoms {O(131) and O(291) [for complexes **1**, **3** and **4**]; O(131) and O(131^{i}) [for complex **2**]} of the compartmental Schiff bases also coordinate to lead(II), but at much longer distances to form equatorial planes. All lead(II)-oxygen bond lengths are comparable to that observed in other complexes with similar structures.[39]

In case of complex **1**, two oxygen atoms of one acetate group coordinates lead(II) centre in axial positions with different Pb-O(acetate) distances {2.394(4) and 2.737(5) Å}. Apparently the acetate may be considered as a chelating bidentate ligand. However, the small value of the bite angle, O(2)-Pb(1)-O(3) [50.5(2)$^{\circ}$], subtended by the two oxygen atoms, O(2) and O(3), suggests that the two oxygen atoms share one axial site, i.e. the acetate group is better thought of as a single entity occupying just one stereochemical site in the coordination sphere of lead(II) instead of as a bidentate ligand. However, because of the vacancies in the equatorial plane, the coordination sphere cannot be described as square pyramidal, rather it is a pentagonal bipyramid with an axial site and an equatorial site unoccupied. In complex **2**, two chlorine atoms, Cl(11) and Cl(11^{i}), coordinate axial positions of lead(II). As can be seen in Fig. 2, the geometry can best be described as a pentagonal bipyramid with one equatorial site unoccupied. Complex **3** is unique in the sense that two oxygen atoms {O(10) and O(3)} of one acetate group bridges nickel(II) and lead (II) {lead(II) by O(3) and nickel(II) through O(1)}. Another interesting feature is that there is another bond from Pb(1) to the thiocyanate S(1) from an adjacent molecule (½-x, ½+y, ½-z) at 3.064(2) Å in complex **3** which leads to the

View Article Online
DOI: 10.1039/C7NJ05148D

formation of a chain, as shown in Fig. 5. It is noteworthy that this bond is on the same side of the equatorial plane as O(1) leading to a very irregular geometry. It may be that the presence of the two ethoxy groups close to the vacant site in the equatorial plane has precluded further bonding in that plane. One axial site is occupied by a chlorine atom, Cl(1), in complex **4**. The geometry can best be considered as a pentagonal bipyramid with an axial and an equatorial site unoccupied (Fig. 4) as in complex **1**.

The Ni(1)O(11)O(31)Pb(1) core is almost planar as the dihedral angle is 9.39° [for complex **1**] and 6.19° [for complex **4**]. In case of complex **2**, Ni(1)O(11)O(11^{i})Pb(1) core is perforce planar as both metals occupy the twofold axis. The dihedral angle is 24.25° and this indicates that the Ni(1)O(11)O(31)Pb(1) core is not planar in complex **3**. The distance between the Ni(1) and Pb(1) is 3.536(7) Å [for complex **1**], 3.464(2) Å [for complex **2**], 3.395(1) Å [for complex **3**] and 3.400(2) Å [for complex **4**].

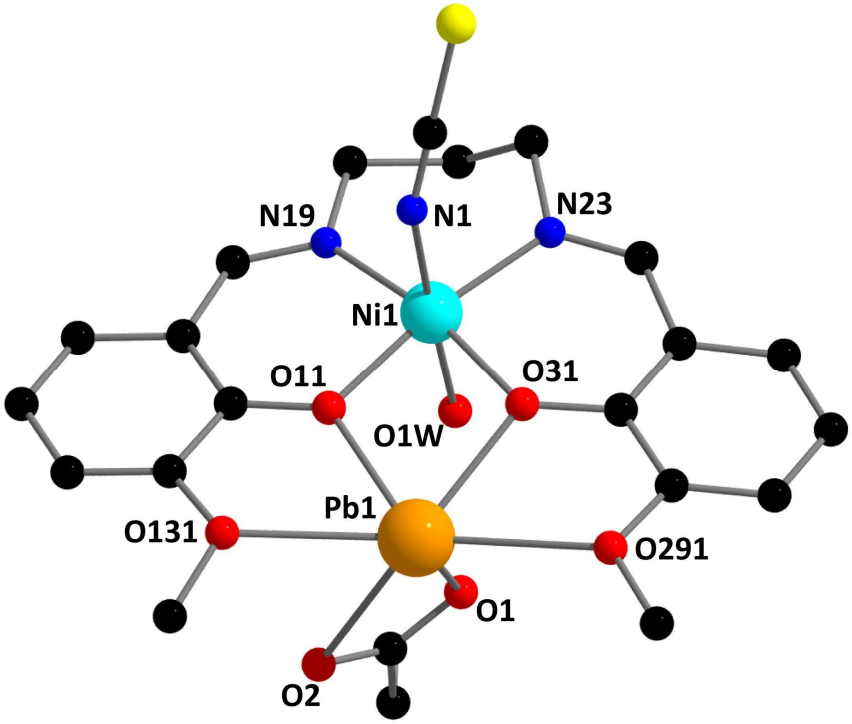

View Article Online
DOI: 10.1039/C7NJ05148D

Fig. 1: Perspective view of complex **1** with selective atom numbering scheme. The solvent DMSO and hydrogen atoms have been omitted for clarity.

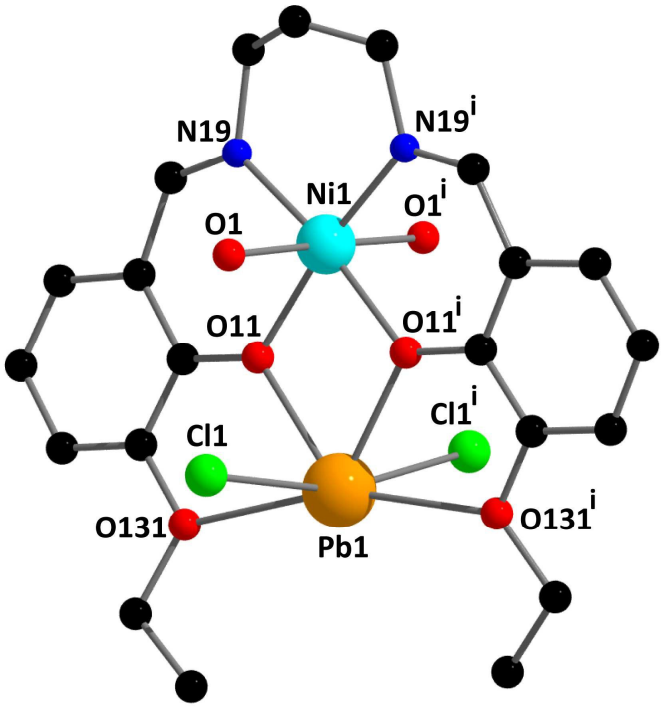

Fig. 2: Perspective view of complex **2** with selective atom numbering scheme. Symmetry element, ^{i} = -x, y, ½-z. Hydrogen atoms have been omitted for clarity.

View Article Online
DOI: 10.1039/C7NJ05148D

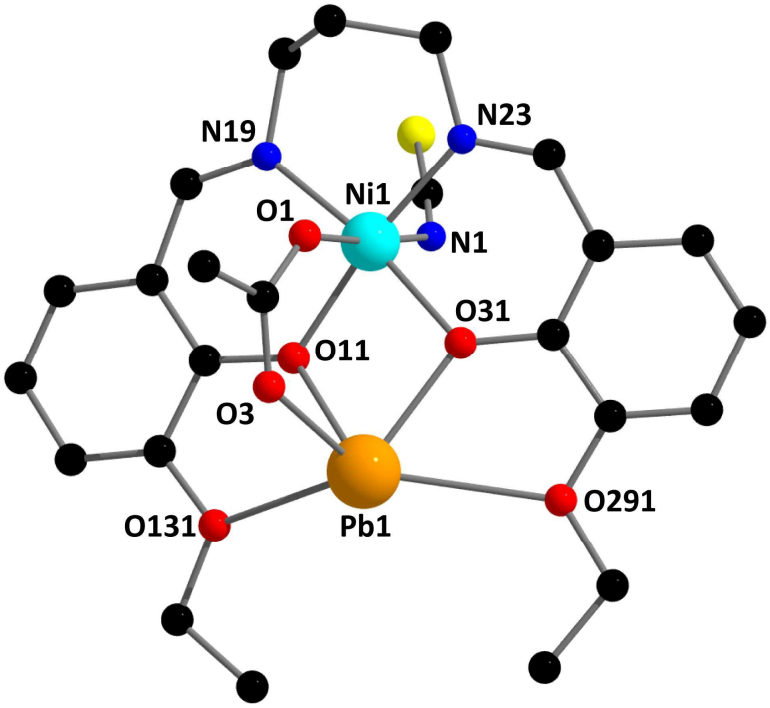

Fig. 3: Perspective view of the asymmetric unit of complex **3** with selective atom numbering scheme. Hydrogen atoms have been omitted for clarity.

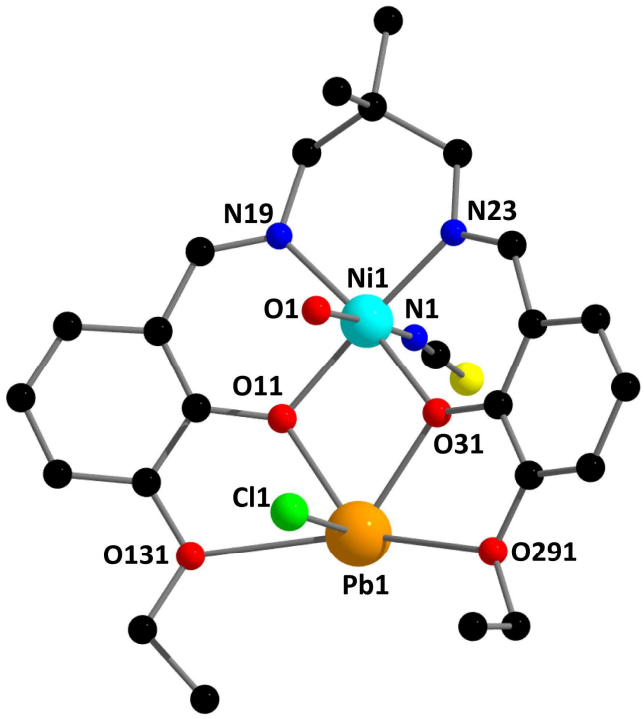

View Article Online
DOI: 10.1039/C7NJ05148D

Fig. 4: Perspective view of complex **4** with selective atom numbering scheme. Hydrogen atoms have been omitted for clarity.

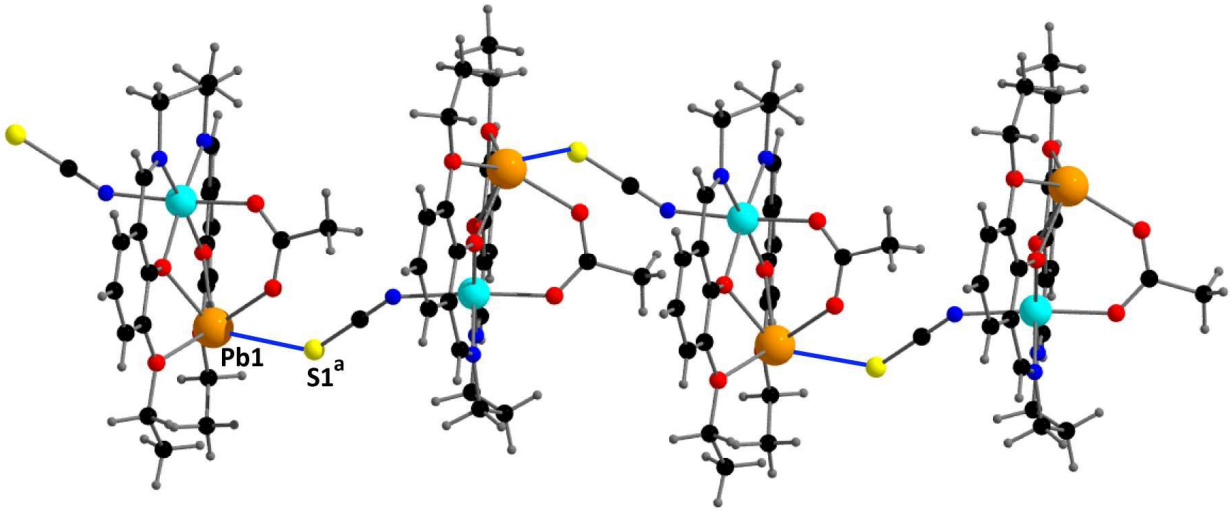

Fig. 5: Perspective view of 1D chain of complex **3** considering a bond between Pb(1) to S(1) at 3.064(2) Å highlighted in violet colour. Symmetry element, [a] = ½-x, ½+y, ½-z.

Table 2: Crystal data and refinement details of complexes **1**-**4**.

Complex	**1**	**2**	**3**	**4**
Formula	$C_{24}H_{31}N_3NiO_8PbS_2$	$C_{21}H_{28}Cl_2N_2NiO_6Pb$	$C_{24}H_{27}N_3NiO_6PbS$	$C_{24}H_{30}ClN_3NiO_5PbS$
Formula Weight	819.55	741.24	751.44	773.92
Temperature(K)	150	150	150	150
Crystal system	Triclinic	Monoclinic	Monoclinic	Triclinic
Space group	$P\bar{1}$	*C2/c*	$P2_1/n$	$P\bar{1}$
a (Å)	10.5264(6)	14.760(3)	12.6526(7)	9.8038(8)
b (Å)	11.3184(6)	12.3947(15)	14.8338(8)	11.9201(11)
c (Å)	12.5352(8)	14.300(3)	13.9646(8)	12.8868(8)
α (°)	86.021(5)	90	90	95.767(6)

View Article Online
DOI: 10.1039/C7NJ05148D

β (°)	71.617(5)	110.72(2)	104.762(6)	104.841(6)
γ (°)	85.853(4)	90	90	111.721(8)
Z	2	4	4	2
d_{calc}(g cm^{-3})	1.928	2.012	1.969	1.947
μ (mm^{-1})	6.821	7.899	7.504	7.302
F (000)	804	1440	1464	756
Total Reflections	9927	5706	15411	5897
Unique Reflections	7843	3387	7177	4369
Observed data [I > 2 σ	7120	2420	5713	3750
No. of parameters	363	162	328	335
R (int)	0.029	0.092	0.058	0.075
R1, wR2 (all data)	0.0520, 0.0997	0.1076, 0.1766	0.0859, 0.1494	0.0893,0.2275
R1, wR2 [I > 2 σ (I)]	0.0452, 0.0958	0.0758, 0.1570	0.0648, 0.1379	0.0761,0.2061

Table 3: Selected bond lengths (Å) of complexes **1**-**4**.

Complex	**1**	**2**	**3**	**4**
Ni(1)-N(19)	2.027(5)	2.032(9)	2.027(7)	2.007(10)
Ni(1)-O(11)	2.047(4)	2.030(7)	2.037(5)	2.005(10)
Ni(1)-O(31)	2.038(4)	-	2.043(5)	2.059(9)
Ni(1)-N(23)	2.051(4)	-	2.047(7)	2.022(10)
Ni(1)-N(1)	2.089(5)	-	2.095(7)	2.048(12)
Ni(1)-O(1W)	2.164(4)	-	-	-
Ni(1)-O(1)	-	2.121(8)	2.084(6)	2.194(9)
Pb(1)-O(11)	2.405(3)	2.306(6)	2.370(5)	2.309(9)
Pb(1)-O(131)	2.696(4)	2.621(7)	2.732(5)	2.684(9)
Pb(1)-O(31)	2.346(4)	-	2.294(5)	2.299(9)

View Article Online
DOI: 10.1039/C7NJ05148D

Pb(1)-O(291)	2.643(4)	-	2.820(5)	2.698(9)
Pb(1)-O(1)	2.737(5)	-	-	-
Pb(1)-O(2)	2.394(4)	-	-	-
Pb(1)-Cl(1)	-	2.939(3)	-	2.637(3)
Pb(1)-O(3)	-	-	2.293(6)	-
Pb(1)-S(1)[a]	-	-	3.064(2)	-

Symmetry element: [a] = -x+½, ½+y, ½-z.

Table 4: Deviation of coordinating atoms from the least square mean plane passing through them and that of nickel(II) from the same plane in complexes **1**, **3** and **4**.

Complex	**Deviations of atoms in Å**				
	O(11)	**O(31)**	**N(23)**	**N(19)**	**Ni(1)**
1	0.055(3)	-0.028(4)	0.051(4)	0.020(5)	0.0573(6)
3	0.012(6)	0.020(6)	0.009(6)	0.018(7)	-0.0171(9)
4	0.047(10)	0.007(10)	0.046(11)	0.001(12	0.085(2)

Supramolecular Interactions

In complex **1**, the water molecule bonded to nickel(II) forms two strong donor hydrogen bonds. Hydrogen atom, H(1), attached to the oxygen atom, O(1W), forms an intramolecular hydrogen bond with an oxygen atom, O(2), of an acetate ligand. Dimensions are O(1W)···O(2) 2.744(5) Å, O(1W)-H(1)···O(2) 174(7)^{o}, H(1)···O(2) 1.90(2) Å. Another hydrogen atom, H(2), attached to the oxygen atom, O(1W), forms an intermolecular hydrogen bond with a symmetry

View Article Online
DOI: 10.1039/C7NJ05148D

related (3-x, 1-y, -z) oxygen atom, O(41), of a DMSO molecule. Dimensions are O(1W)···O(41) 2.808(5) Å, O(1W)-H(2)···O(41) 173(7)°, H(2)···O(41) 1.96(2) Å. The hydrogen bonding interactions are shown in Fig. 6.

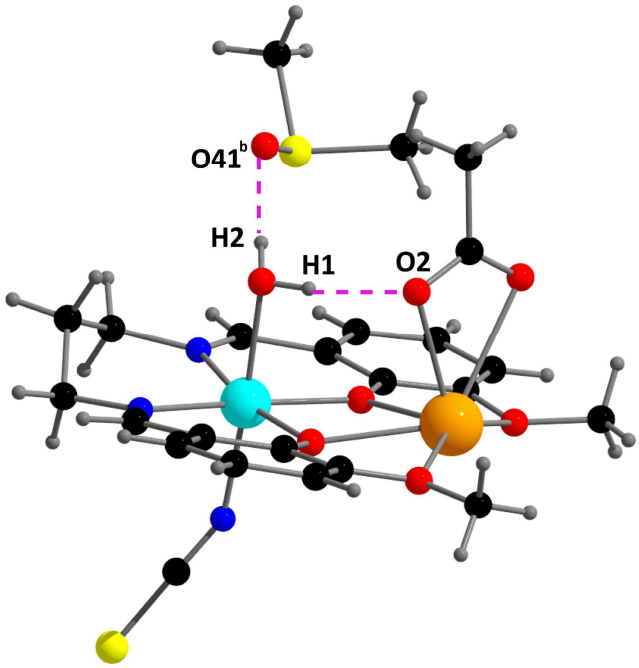

Fig. 6: Perspective view of hydrogen bonding interaction in complex **1**. Symmetry element [b] = 3-x, 1-y, -z.

In complex **2**, the water molecules bonded to the nickel(II) form hydrogen bonds to the chlorine atoms bonded to the lead(II). Hydrogen atom, H(1), attached to oxygen atom, O(1), forms an intramolecular hydrogen bond with a chlorine atom, Cl(1), bonded to Pb(1). Dimensions are O(1)···Cl(1) 3.161(8) Å, O(1)-H(1)···Cl(1) 160(8)°, H(1)···Cl(1) 2.34(4) Å. Another hydrogen atom, H(2), attached to oxygen atom, O(1), forms an intermolecular hydrogen bond with a symmetry (x,2-y,1/2+z) related chlorine atom, Cl(1). Dimensions are O(1)···Cl(1) 3.225(8)

View Article Online
DOI: 10.1039/C7NJ05148D

Å, O(1)-H(2)···Cl(1) 160(9)°, H(2)···Cl(1) 2.41(4) Å. These interactions lead to the formation of 1D chain shown in Fig. 7.

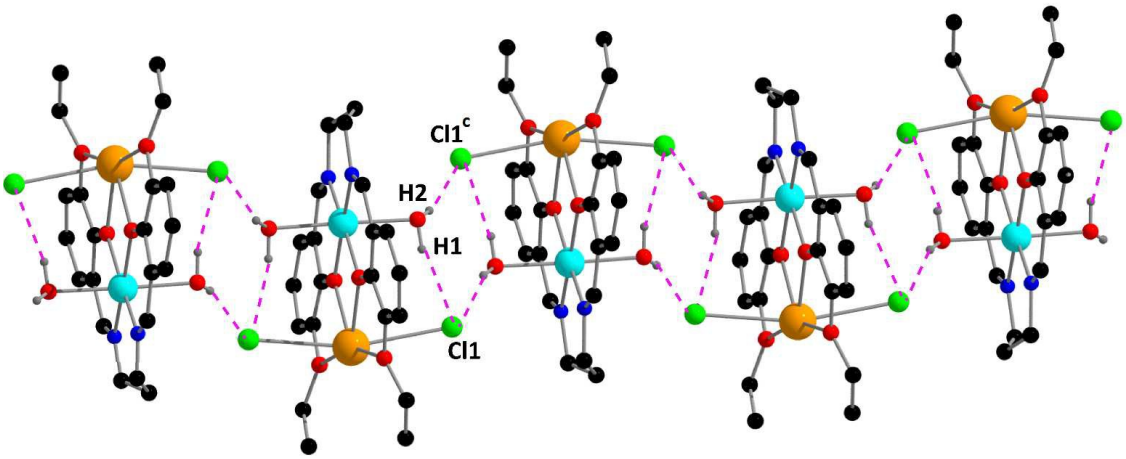

Fig. 7: Perspective view of 1D chain formed by hydrogen bonding interactions in complex **2**. Only relevant atoms have been shown for clarity. Symmetry transformation: ^{c} = x,2-y,1/2+z.

In complex **3**, no significant H-bonding interactions are observed. In complex **4**, two hydrogen bonding interactions are observed. Hydrogen atom, H(1), attached to the oxygen atom, O(1), forms an intermolecular hydrogen bond with a symmetry (1-x,1-y,-z) related chlorine atom, Cl(1). Dimensions are H(1)···Cl(1) 2.40(2) Å, O(1)-H(1)···Cl(1) 170(4)°, O(1)···Cl(1) 3.256(11) Å. Hydrogen atom, H(2), attached to the oxygen atom, O(1), forms an intramolecular hydrogen bond to Cl(1), but this is rather weak compared to the intermolecular hydrogen bond. Dimensions are H(2)···Cl(1) 2.88(2) Å, O(1)-H(2)···Cl(1) 113(12)°, O(1)···Cl(1) 3.308(12) Å. These interactions form a supramolecular dimer shown in Fig. 8.

View Article Online
DOI: 10.1039/C7NJ05148D

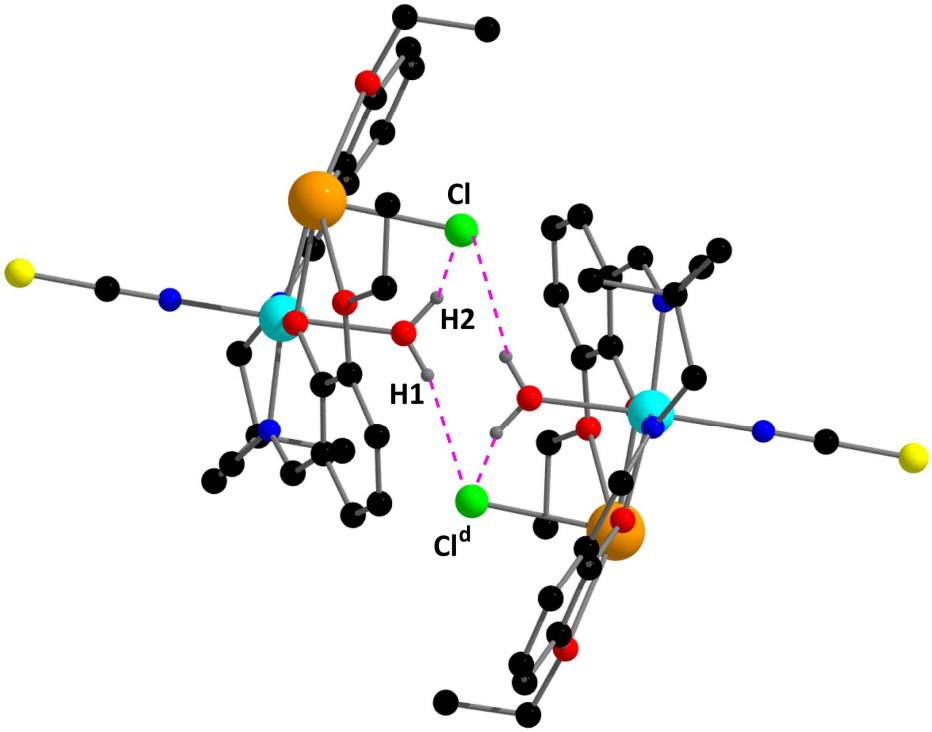

Fig. 8: Perspective view of hydrogen bonding interactions in complex **4**. Only the relevant atoms have been shown for clarity. Symmetry transformation: ^{d} = 1-x,1-y,-z.

IR and electronic spectra

Distinct bands due to the azomethine (C=N) groups at 1632 cm^{-1}, 1628 cm^{-1},1632 cm^{-1} and 1637 cm^{-1} are routinely noticed in the IR spectra of complexes **1**-**4** respectively (Figures S1-S4) {ESI (Electronic Supplementary Information)}.[40] A strong band at 2069 cm^{-1}, 2101 cm^{-1} and 2097 cm^{-1} indicate the presence of terminal N-bonded thiocyanate in complexes **1**, **3** and **4** respectively.[41] Broad bands at 3379 cm^{-1}, 3406 cm^{-1} and 3499 cm^{-1} indicate the presence of the O-H stretching frequency of water molecule in complexes **1**, **2** and **4** respectively.[42] Absorptions ~1463 and at 1416 cm^{-1} are attributed to asymmetric and symmetric (C=O) stretching frequency of the acetate group, respectively in complex **1** and **3**.[43]

View Article Online
DOI: 10.1039/C7NJ05148D

Electronic spectra of the complexes (Figures S5-S8) {ESI (Electronic Supplementary Information)} display five bands around 250 nm, 270 nm, 350 nm, 560 nm and 820 nm. Absorption bands around 560 nm may be assigned as $^3T_{1g}(F) \leftarrow {}^3A_{2g}(F)$, whereas bands at 820 nm may be assigned as $^3T_{2g}(F) \leftarrow {}^3A_{2g}(F)$ respectively.[44] The higher energy d-d band, $^3T_{1g}(P) \leftarrow {}^3A_{2g}(F)$, cannot be observed as it is obscured by a strong charge transfer transition (~350 nm) in each case.[45] The UV absorption bands around 270 nm may be assigned to intra ligand n-π* transitions.[46] Bands around 250 nm may be attributed to π-π* transitions.[47] Electronic spectra of the ligands are shown in (Figures S9-S11) {ESI (Electronic Supplementary Information)}. All complexes exhibit fluorescence (Fig. S12). The fluorescence data are listed in Table 5 (without solvent correction). The fluorescence spectra of H_2L^1, H_2L^2 and H_2L^3 (Fig. S13) were also recorded (Excitation wavelengths were 329, 328 and 330 nm respectively, and emission wave lengths were 440 nm, 440 nm and 442 nm respectively) and compared with that of the complexes (Table 5). There is a clear shift in emission maxima towards high energy region. The fluorescence intensity also decreases in complexes probably due to the presence of paramagnetic nickel(II) centres in each case. These are assigned as intra-ligand (π-π^*) fluorescence.[47] Mean lifetimes (τ_{avg}) of the exited states are listed in Table 5. Decay profiles are shown in Fig. 9.

View Article Online
DOI: 10.1039/C7NJ05148D

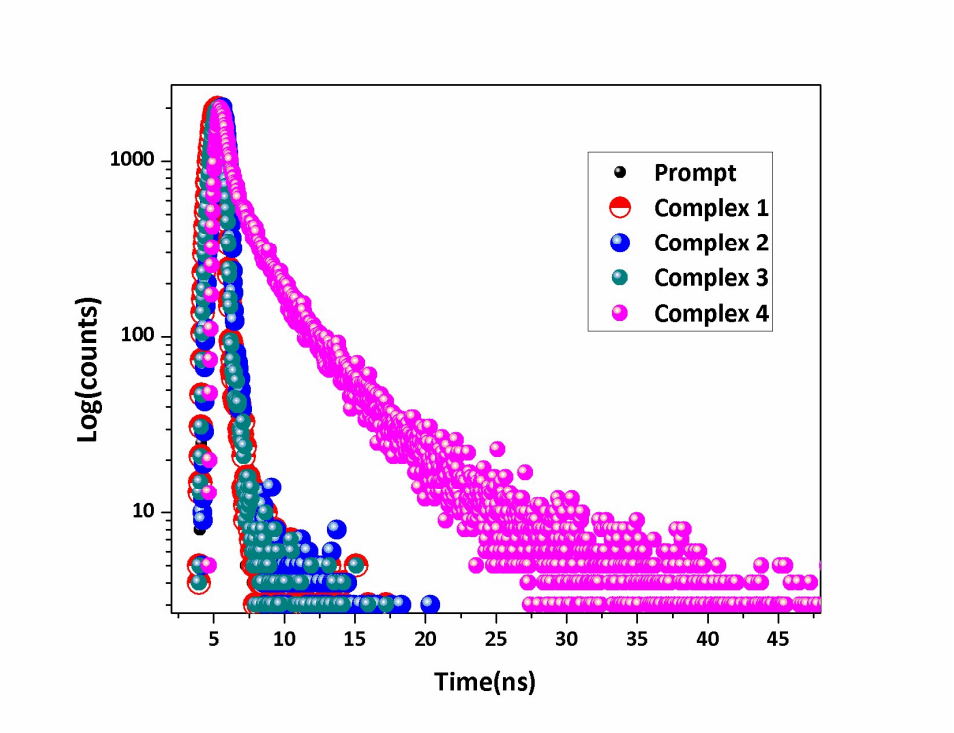

Fig. 9: Lifetime decay profile of complexes **1**-**4**.

Table 5: Photophysical data for complexes **1**-**4**.

Complex	Excitation (nm)	Emission (nm)	A_1 (%)	τ_1(ns)	A_2 (%)	τ_2(ns)	τ_{avg} (ns)	χ^2
1	350	391	67.38	1.17	32.62	5.67	4.3	1.01
2	350	390	51.43	1.83	48.57	4.78	3.9	1.09
3	350	390	61.34	2.15	38.66	4.38	3.4	1.21
4	348	390	64.36	2.84	35.64	5.91	4.5	1.11

View Article Online
DOI: 10.1039/C7NJ05148D

Hirshfeld surfaces

Hirshfeld surfaces of complexes **1**-**4**, mapped over d_{norm} (range of -0.1 to 1.5 Å), shape index and curvedness, are illustrated in Fig. 10. Transparent surfaces are used so that molecular moieties (around which the surfaces are calculated) can be visualised clearly. Red spots on the d_{norm} surface (Fig. 10) indicate the interaction between sulphur and hydrogen atoms. O···H, N···H and Cl···H contacts are also observed in the Hirshfeld surfaces as smaller visible spots of light colour indicating weaker and longer contact. Distinct spikes in 2D fingerprint plot (Fig. 11) indicate intermolecular interactions, e.g. S···H/H···S, Cl···H/H···Cl or O···H/H···O interactions etc. Relative contributions to the Hirshfeld surface area for the various intermolecular contacts in complexes **1**-**4** are shown in Fig. 12.

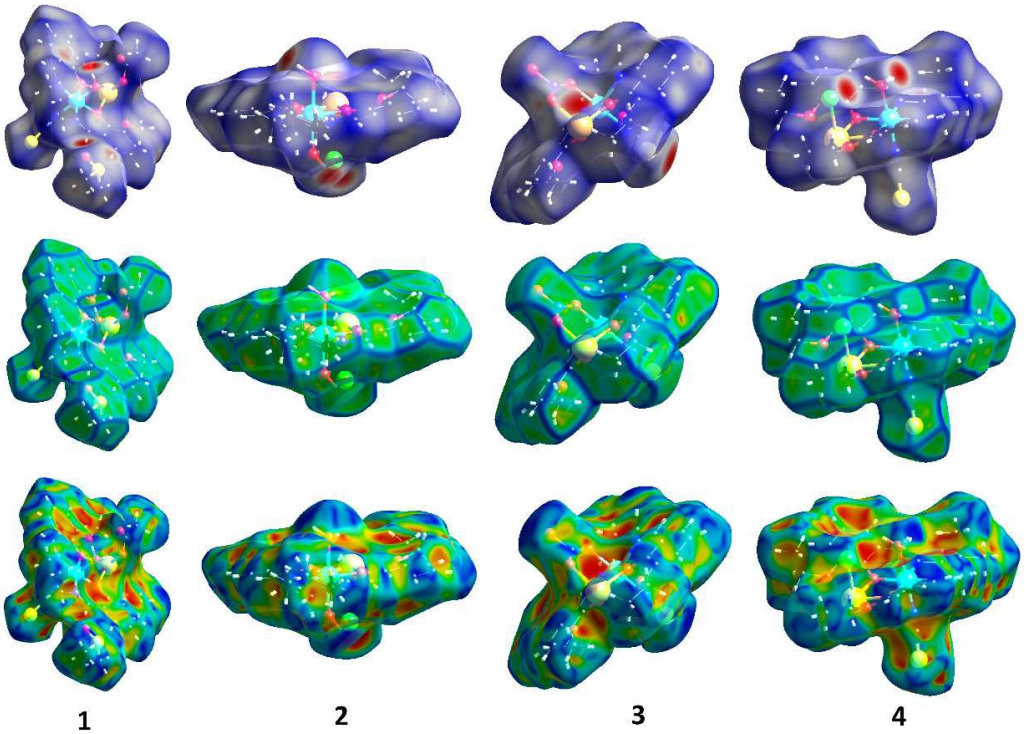

Fig. 10: Hirshfeld surfaces mapped with d_{norm} (top), shape index (middle) and curvedness (below) for complexes **1**-**4**.

View Article Online
DOI: 10.1039/C7NJ05148D

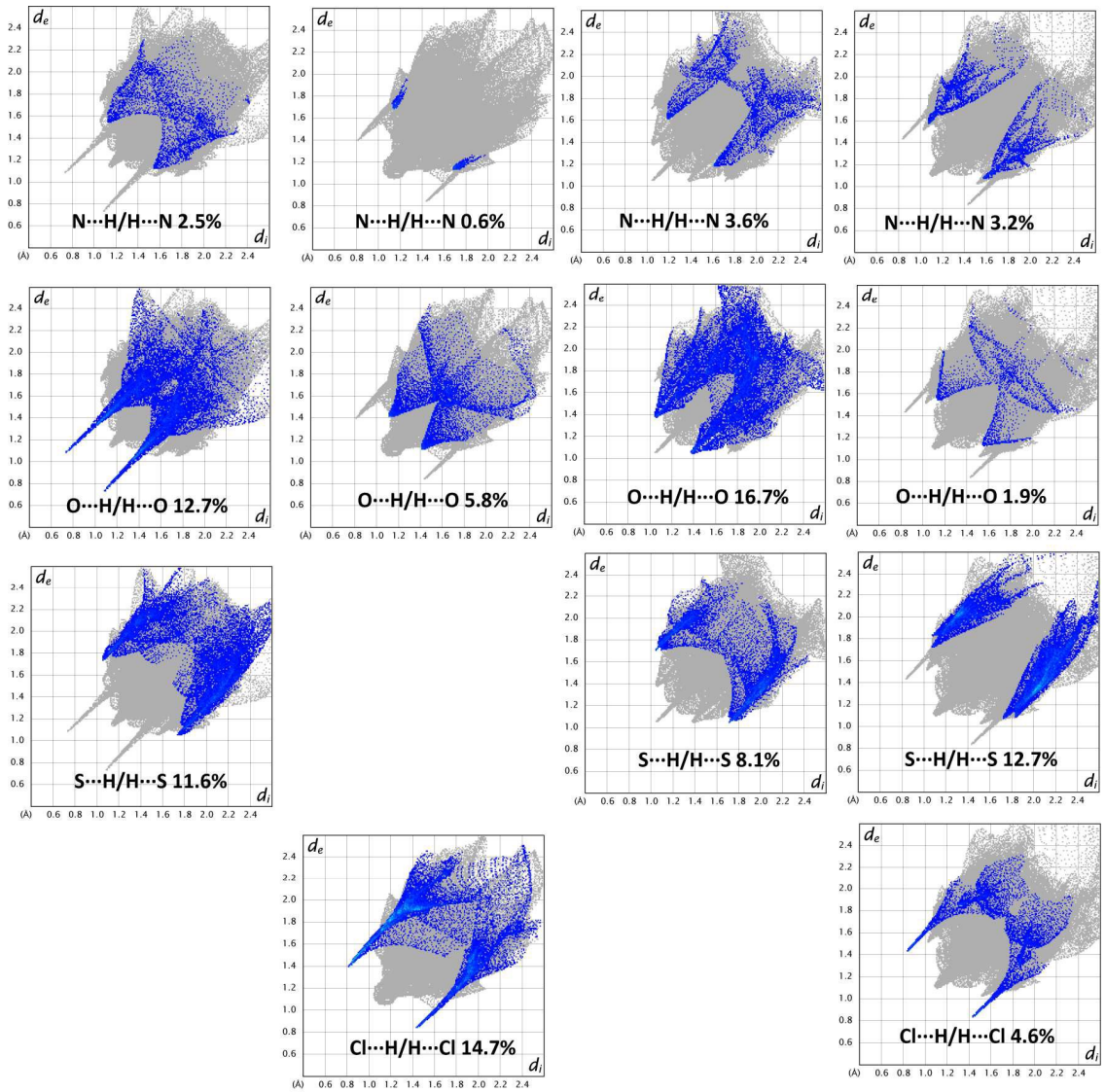

Fig. 11: Fingerprint plot: Different contacts contributed to the total Hirshfeld Surface area of complexes **1**-**4**.

View Article Online
DOI: 10.1039/C7NJ05148D

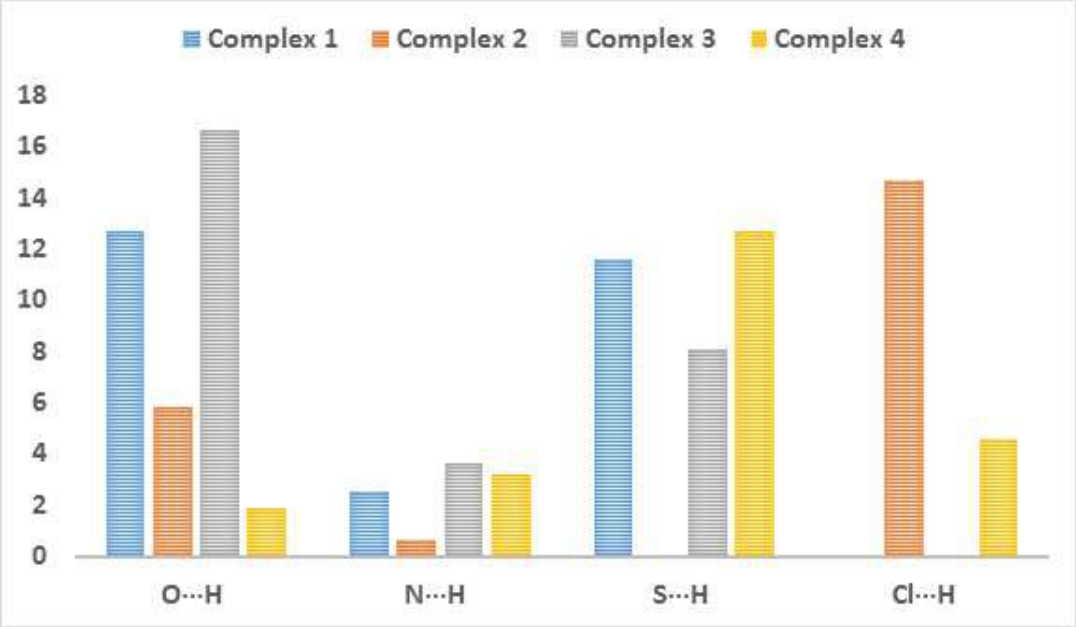

Fig. 12: Relative contributions to the Hirshfeld surface area for the various intermolecular contacts in complexes **1**-**4**.

Theoretical study of the supramolecular assemblies

The theoretical study has been focused on the analysis of the remarkable supramolecular assemblies observed in the solid state of complexes **1** and **3**, directing our attention to the tetrel bonding interactions. Particularly in complex **1**, the Pb···N interactions have been analysed that promote the formation of self-assembled dimers in the solid state. Moreover, in complex **3**, the Pb···S interactions have been studied that govern the formation of infinite 1D chains in its solid state architecture.

Self-complementary Pb···N contacts are responsible for the formation of self-assembled dimers in complex **1** (Fig. 13a) that are interconnected to other dimers by weak van der Waals interactions. In order to rationalize the donor-acceptor properties of the Pb(II) complex, the

View Article Online
DOI: 10.1039/C7NJ05148D

molecular electrostatic potential (MEP) surface of complex **1** has been computed which is represented in Fig. 13b. In the MEP surface the most positive part corresponds to the hydrogen atom of the coordinated water molecule (not shown in the orientation used to represent the MEP surface in Fig 13b) that does not form the intramolecular O-H···O-H bond with the acetate ligand (Fig 13c). However, this hydrogen atom forms an intramolecular hydrogen bond with a co-crystalized DMSO molecule and, consequently, it is not available to participate in the formation in supramolecular assemblies. The MEP value at the void space of the lead(II) atom is positive (+25 kcal/mol) and the most negative part of the molecule is located at the nitrogen atom of the pseudohalide ligand. The directionality of the lone pair of nitrogen atom and the lead(II) σ-hole is ideal for the formation of the self-assembled dimers in complex **1**. The interaction energy is large and negative (ΔE_1 = −40.8 kcal/mol) and thus indicates a very strong binding motif in the crystal structure. This large binding energy is due to the existence of additional interactions (π-stacking and hydrogen bonds) that are further discussed below.

View Article Online
DOI: 10.1039/C7NJ05148D

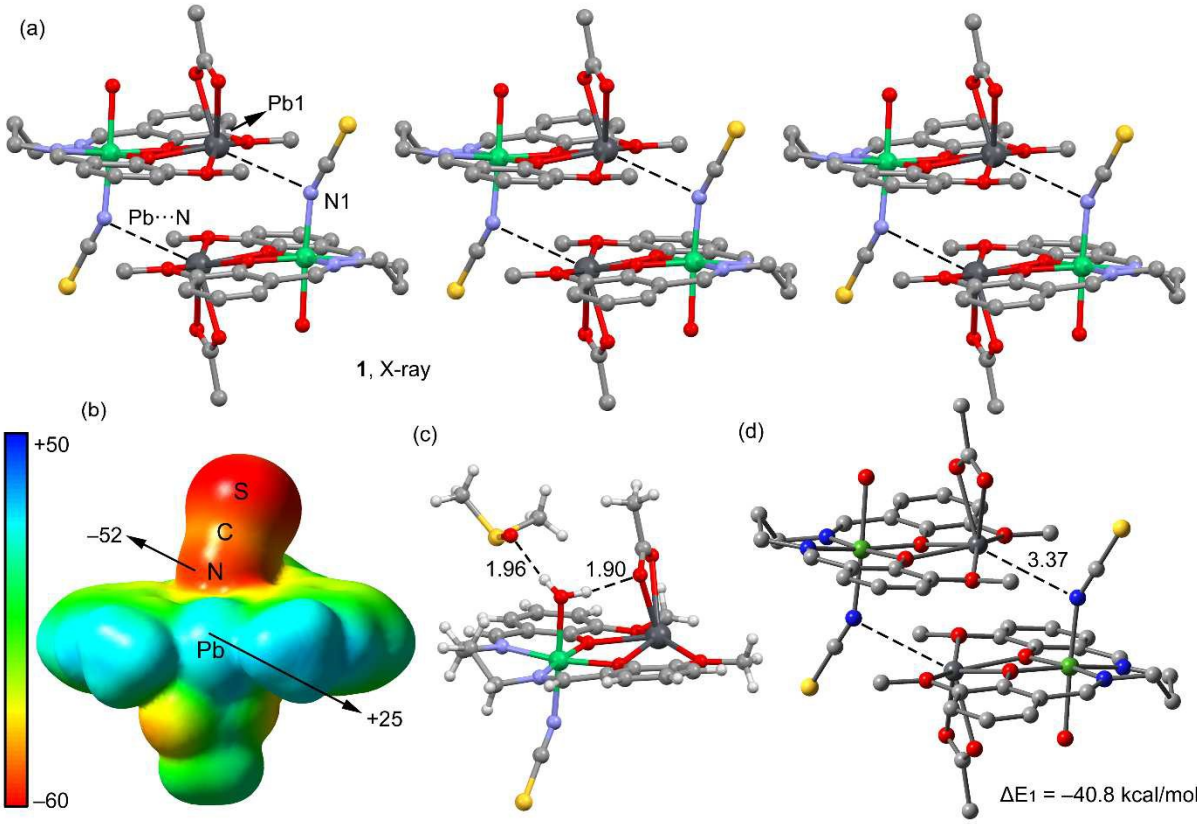

Fig. 13: (a) Partial view of the X-ray structure of complex **1** using a centrosymmetric dimeric model using molecules x,y,z and 2-x, 1-y, 1-z. (b) MEP plotted onto the van der Waals surface (0.01 a.u.) of complex **1**. The MEP values at selected points of the surface are indicated. (c) Detail of the hydrogen bonding interactions involving the water molecule. (d) The centrosymmetric dimeric fragment used to evaluate the tetrel bonding interactions.

In complex **2**, tetrel bonding interactions are not observed. The MEP surface given in Fig. 14a reveals that the presence of both chlorido ligands at the lead(II) centre along with the steric hindrance of the ethoxy substituents excludes the lead(II) from interacting with electron rich atoms.

View Article Online
DOI: 10.1039/C7NJ05148D

The most negative part of the surface corresponds to the chloride ligands and the most positive part to the hydrogen atom of the coordinated water molecule (+50 kcal/mol, Fig. 14a). Therefore, the most representative assembly of this compound in the solid state is the infinite 1D chains depicted in Fig. 14b.

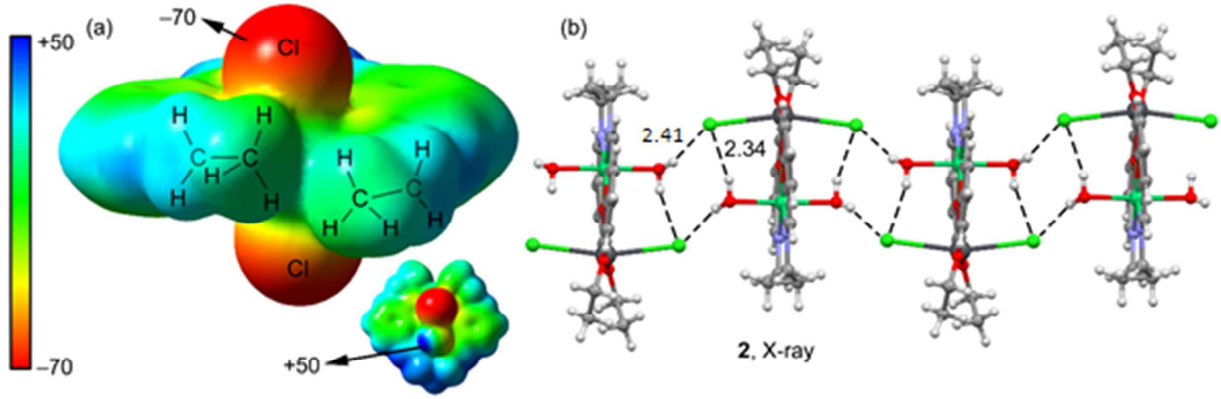

Fig. 14: (a) MEP plotted onto the van der Waals surface (0.01 a.u.) of complex **2**. The MEP values at selected points of the surface are indicated. (b) Partial view of the hydrogen bonding network in complex **2**. Distances in Å.

In complex **3**, the theoretical study is focused on the computation of the energy of the Pb···S interactions responsible for the formation of the infinite 1D supramolecular chain shown in Fig. 15a. Two interactions are likely responsible for the formation of this assembly, Pb···S tetrel bonding and C-H···π interactions. The MEP surface shown in Fig. 15b reveals that the lead(II) is accessible for interacting with electron rich atoms and presents a large σ-hole (+50 kcal/mol). The MEP value at the sulphur atom of the thiocyanate ligands is -57 kcal/mol. The interaction energy of a dimer extracted from the infinite 1D chain (Fig. 15c) is very large (ΔE_2 = −13.7 kcal/mol) because of the contribution of both C-H···π and tetrel bonding interactions.

View Article Online
DOI: 10.1039/C7NJ05148D

Remarkably, the sulphur atom of the pseudohalide is located exactly at the σ-hole position of the lead(II), in good agreement with the MEP analysis and confirming the directionality of the interaction. In order to evaluate the contribution of each interaction an additional theoretical model has been computed where the acetate ligand has been replaced by a formate ligand. In this model the C-H···π interaction is not established and consequently the binding energy (ΔE_3 = -13.5 kcal/mol) corresponds to the contribution from the tetrel bonding interaction and the difference (-0.2 kcal/mol) is the contribution of the C-H···π interaction that is very weak, likely due the fact that the positive hydrogen atom is not pointing to the π-system of the arene. Therefore, the tetrel bonding is the main force governing the formation of the infinite 1D chain in the solid state of complex **3**.

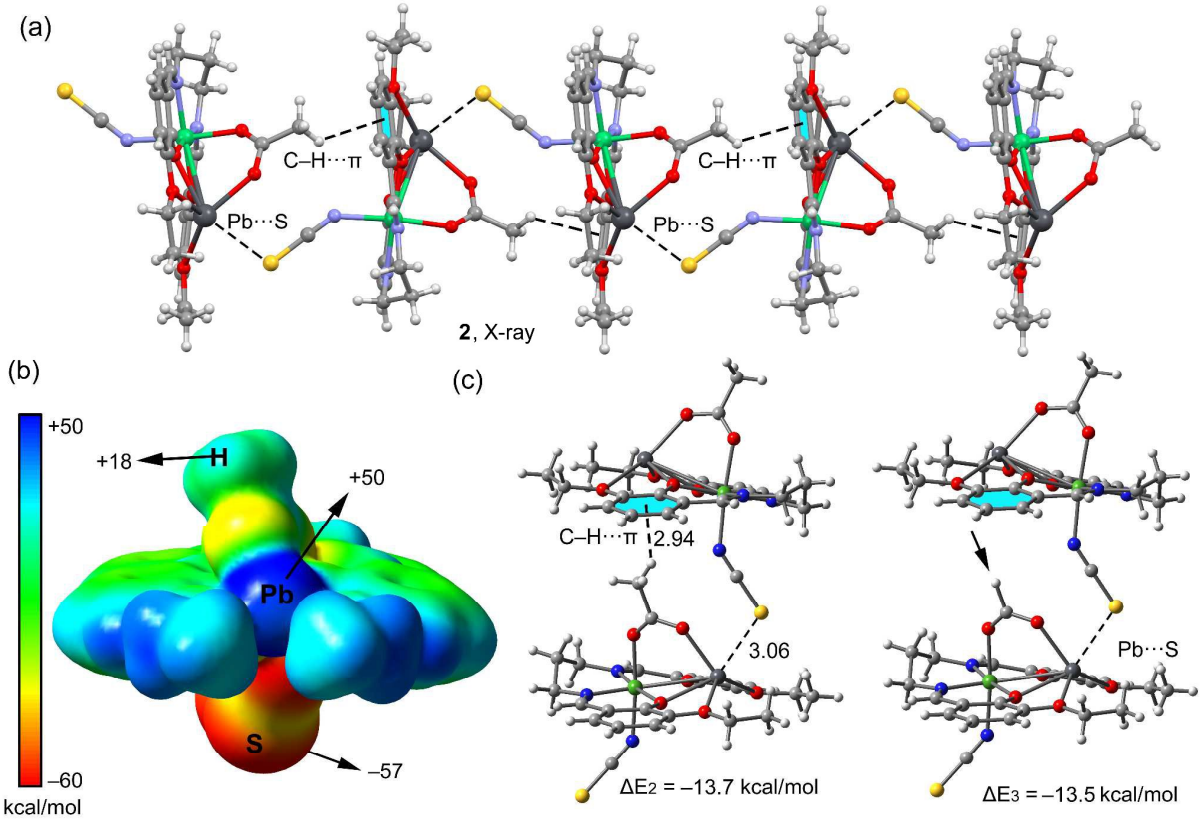

View Article Online
DOI: 10.1039/C7NJ05148D

Fig. 15: (a) Partial view of the X-ray structure of complex **3**. (b) MEP plotted onto the van der Waals surface (0.01 a.u.) of complex **3**. The MEP values at selected points of the surface are indicated (c,d). Theoretical models used to evaluate the tetrel bonding and C-H···π interactions.

The MEP surface of complex **4** is represented in Fig. 16a. The lead(II) is exposed and thus available for establishing tetrel bonding interactions, however the MEP value at the lead(II) is significantly smaller (+8.0 kcal/mol) than the MEP value at the lead(II) in complexes **1** and **3** (+25 kcal/mol and +45 kal/mol, respectively). This is likely due to the orientation of the anionic thiocyanate ligand that is tilted toward the lead(II), thus influencing its MEP value. Consequently, tetrel bonding interactions are not present in the solid state of complex **4**. In contrast, π···π interactions are established (Fig. 16b), where carbon atoms of the aromatic ring are close to lead(II) (dashed lines in Fig. 16b), also preventing the interaction with additional electron rich atoms.

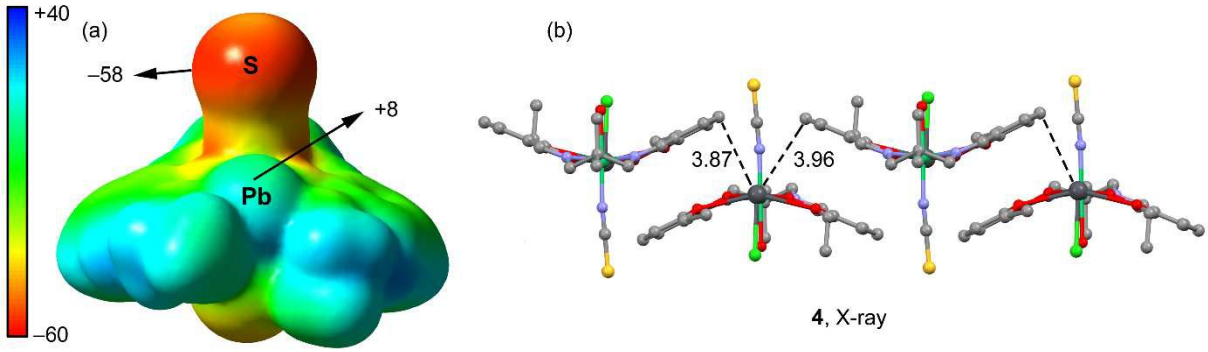

Fig. 16: (a) MEP plotted onto the van der Waals surface (0.01 a.u.) of complex **4**. The MEP values at selected points of the surface are indicated. (b) Partial view of the X-ray structure of complex **4** showing π···π assemblies. Distances in Å.

View Article Online
DOI: 10.1039/C7NJ05148D

Finally, the Bader's theory of "atoms in molecules", has been used which provides an unambiguous definition of chemical bonding, to further describe the non-covalent tetrel bonding interactions described above for complexes **1** and **3**. The AIM theory has been effectively utilized to characterize a great variety of interactions.[48,16b,c,18d] In Fig. 17(a), the AIM analysis of the self-assembled dimer of complex **1** has been shown and the combined C-H···π interaction and tetrel bonding of complex **3**, shown in Fig. 17(b). The Pb···N interaction in complex **1** is confirmed by the presence of a bond CP and a bond path connecting the nitrogen atom of pyridine to the lead(II). In this particular dimer, the distribution of critical points and bond paths is very complicated due to the presence of additional interactions (π-stacking and hydrogen-bonding). Therefore, only the bond CPs that characterize the interactions involving lead(II) are represented (Fig. S14) for a full representation of the AIM distribution of CPs). A bond CP and bond path can be observed connecting both lead(II), thus revealing the existence of a metallophilic interaction between both tetrel atoms. Regarding the dimer of complex **3**, (Fig. 17b) the Pb···S interaction is characterized by the presence of a bond CP and bond path interconnecting both atoms. Moreover, the existence of the ancillary C-H···π interaction is confirmed by the presence of a bond CP and bond path that connect one hydrogen atom of the acetato ligand to one carbon atom of the aromatic ring. The value of the Laplacian of the charge density computed at the bond critical points in both assemblies is positive, as is common in closed-shell interactions.

View Article Online
DOI: 10.1039/C7NJ05148D

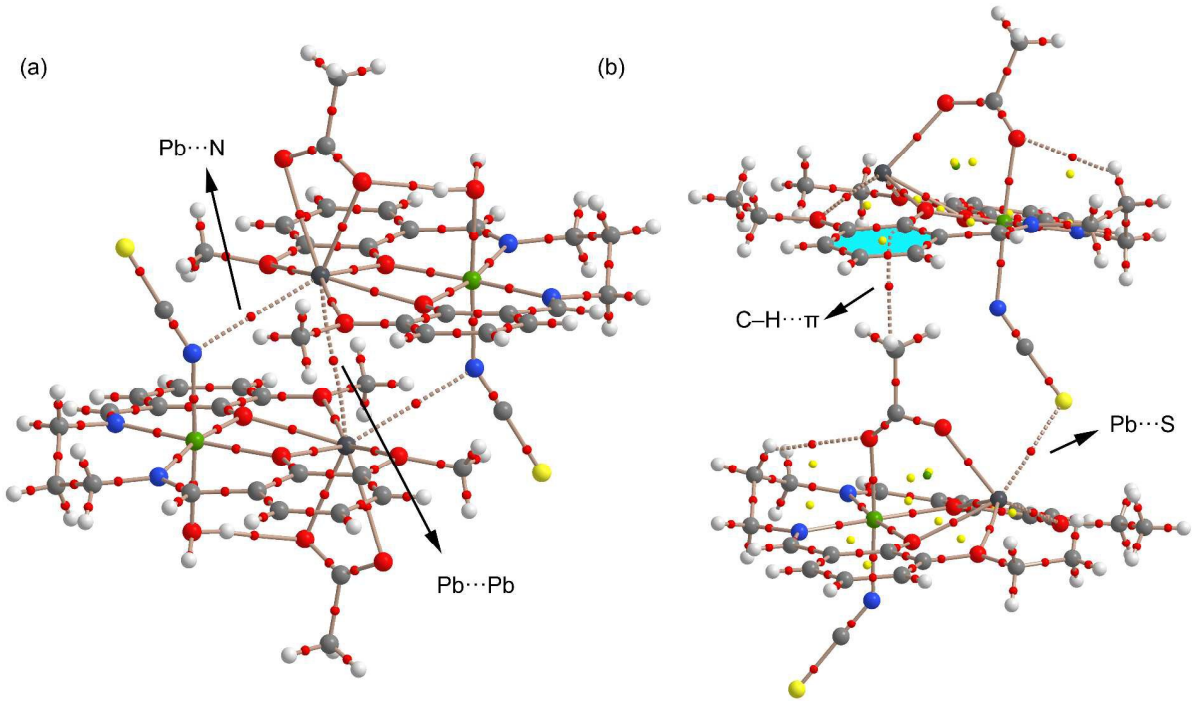

Fig. 17: AIM analyses of the dimers of complex **1** in (a) and complex **3** in (b). Bond, ring and cage critical points are represented by red, yellow and green spheres, respectively. The bond paths connecting bond critical points are also represented by dashed lines. For complex **1**, only the bond CPs and bond paths that characterize the tetrel and Pb···Pb interactions are represented for the sake of clarity. See Fig. S14 {ESI (Electronic Supplementary Information)} for the complete AIM analysis.

Concluding Remarks

In conclusion, we report the syntheses and structural characterization of four new heterodinuclear nickel(II)/lead(II) complexes with N_2O_4 donor compartmental Schiff base ligand. Complexes **1** and **3** exhibit relevant tetrel bonding interactions in the solid state that generate interesting supramolecular assemblies. They have been described and characterized using M06-2x/def2-TZVP calculations including their energetic features. In general, these non-covalent

View Article Online
DOI: 10.1039/C7NJ05148D

Pb···N interactions are strong due to electrostatic effects, as shown by molecular electrostatic potential calculations. We have also rationalized the absence of tetrel bonding interactions in complexes **2** and **4** using MEP surfaces plotted onto the van der Waals surface. Our results might be important to understand the X-ray structure of organic–inorganic materials systems that contain hemidirectionally coordinated lead(II) centres and organic aromatic molecules.

Notes and References

Electronic supplementary information (ESI) available: Table S1 and Fig. S1-S14.

CCDC 1580464-1580467 contain the supplementary crystallographic data for complexes **1**-**4** respectively. These data can be obtained free of charge via www.ccdc.cam.ac.uk/data_request/cif, or by emailing data_request@ccdc.cam.ac.uk, or by contacting The Cambridge Crystallographic Data Centre, 12, Union Road, Cambridge CB2 1EZ, UK; fax: +44 1223 336033.

Acknowledgments

A.B. and A.F. thank the DGICYT of Spain (project CTQ2014-57393-C2-1-P). We thank the CTI (UIB) for computational facilities. We thank the EPSRC (U.K.) and the University of Reading for funds for the diffractometer.

References

1 (a) R. M. Harrison and D. R. H. Laxen, *Lead Pollution*, Chapman & Hall, London, 1981; (b) J. M. Christensen and J. Kristiansen, *In: Handbook of Metals in Clinical and Analytical Chemistry* (Eds.: H. G. Seiler, A. Sigel, H. Sigel), Marcel Dekker, New York, 1994, pp. 425-440; (c) B. P. Lanphear, D. A. Burgoon, S. W. Rust, S. Eberly and W. Galke, *Environmental Res.,* 1998, **76**, 120-130; (d) T.

View Article Online
DOI: 10.1039/C7NJ05148D

G. Spiro and W. M. Stigliani, *Chemistry of the Environment*, Prentice Hall, Upper Saddle River, NJ, 1996; (e) F. Cuenot, M. Meyer, A. Bucaille and R. Guilard, *J. Mol. Liquids*, 2005, **118**, 89-99; (f) R. A. Goyer, *In Handbook on Toxicity of Inorganic Compounds* (Eds.: H. G. Seiler, H. Sigel, A. Sigel), Marcel Dekker: New York, 1988; (g) J. J. Chisholm, *Sci. Am*., 1971, **224**(**2**), 15-23.

2 (a) A. Morsali and A. R. Mahjoub, *Helv. Chim. Acta,* 2004, **87**, 2717-2722; (b) H. Fleischer and D. Schollmeyer, *Inorg. Chem*., 2004, **43**, 5529-5536; (c) D. L. Reger, T. D. Wright, C. A. Little, J. J. S. Lamba and M. D. Smith, *Inorg. Chem*., 2001, **40**, 3810-3814; (d) R. D. Hancock, J. H. Reibenspies and H. Maumela, *Inorg. Chem*., 2004, **43**, 2981-2987; (e) C. Platas-Iglesias, D. Esteban-Gomez, T. Enriquez-Perez, F. Avecilla, A. de Blas and T. Rodriguez-Blas, *Inorg. Chem*., 2005, **44**, 2224-2233.

3 (a) F. Cheng, J. Liang, Z. Tao and J. Chen, *Adv. Mater.,* 2011, **23**, 1695-1715; (b) L. Zhang, Y.-Y. Qin, Z.-J. Li, Q.-P. Lin, J.-K. Cheng, J. Zhang and Y.-G. Yao, *Inorg. Chem.,* 2008, **47**, 8286-8293; (c) C. A. Randall, A. S. Bhalla, T. R. Shrout and L. E. Cross, *J. Mater. Res*., 1990, **5**, 829-834. (d) J. Masek, *J. Phys. C: Solid State Phys*., 1988, **21**, 2821-2827; (e) A. Olvera, G. Shi, H. Djieutedjeu, A. Page, C. Uher, E. Kioupakis and P. F. P. Poudeu, *Inorg. Chem.,* 2015, **54**, 746-755.

4 (a) C. L. Seaton, J. Lasman and D. R. Smith, *Toxicol. Appl. Pharmacol.,* 1999, **159**, 153-160; (b) D. A. Cory-Slechta, B. Weiss and C. Cox, *J. Pharmacol. Exp. Ther.,* 1987, **243**, 804-813; (c) D. E. Glotzer, K. A. Freedberg, and H. Baucher, *Med. Decision Making*; 1995, **15(1)**, 13-24; (d) D. E. Glotzer and H. Baucher, *Pediatrics,* 1992, **89**, 614-618. (e) CDC (Centers for Disease Control), *Preventing Lead Poisoning in Young Children. A statement by The Centers for Disease Control-*

View Article Online
DOI: 10.1039/C7NJ05148D

October, 1991. U.S Department of Health and Human Services/Public Health Service/Centers for Disease Control; (f) M. E. Markowitz and J. F. Rosen, *J. Pediatr*., 1991, **119(2)**, 305-310.

5 (a) S.-R. Fan and L.-G. Zhu, *Inorg. Chem*., 2007, **46**, 6785-6793; (b) R. Ferreirs-Martínez, D. Esteban-Gomez, E. Toth, A. de Blas, C. Platas-Iglesias and T. Rodríguez-Blas, *Inorg. Chem*., 2011, **50**, 3772-3784; (c) J. M. Ratcliffe, *Lead in Man and Environment*; John Wiley & Sons: New York, 1981; (d) M. D. J. J. Chisolm Jr, *J. Pediatr*., 1968, **73**, 1-38.

6 (a) T.-T. Liu, J. Liang, Y.-B. Huang and R. Cao, *Chem. Commun.,* 2016, **52**, 13288-13291; (b) Y. Huang, T. Liu, J. Lin, J. Lü, Z. Lin, and Rong Cao, *Inorg. Chem*., 2011, **50**, 2191-2198; (c) E. C. Constable, G. Zhang, C. E. Housecroft, M. Neuburger and J. A. Zampese, *CrystEngComm*, 2010, **12**, 1764-1773.

7 (a) C. T. Lyons, T. Daniel P. Stack, *Coord. Chem. Rev.,* 2013, **257**, 528-540; (b) P. G. Cozzi, *Chem. Soc. Rev.,* 2004, **33**, 410-421; (c) C. Baleizao, H. Garcia, *Chem. Rev.*, 2006, **106**, 3987-4043; (c) E. C. Constable, G. Zhang, C. E. Housecroft and J. A. Zampese, *Dalton Trans.*, 2010, **39**, 1941-1947.

8 (a) X. Yang, B. P. Hahn, R. A. Jones, K. J. Stevenson, J. Steven Swinnea and Q. Wu, *Chem. Commun*., 2006, 3827-3829; (b) A. C. Sudik, A. R. Millward, N. W. Ockwig, A. P. Coˆte´, J. Kim and O. M. Yaghi, *J. Am. Chem. Soc*., 2005, **127**, 7110-7118; (c) A. V. Davis and K. N. Raymond, *J. Am. Chem. Soc*., 2005, **127**, 7912-7919.

9 (a) B. Dede, F. Kripcin and M. Cengiz, *J. Hazard. Mater*., 2009, **163**, 1148-1156; (b) G. Cote and A. Jakubiak, *Hydrometallurgy,* 1996, **43**, 277-286.

View Article Online
DOI: 10.1039/C7NJ05148D

10 (a) T. Nakajima, I. Shimizu, K. Kobayashi and Y. Wakatsuki, *Organometallics*, 1998, **17**, 262-269; (b) A. J. Tasiopoulos, T. A. O' Brien, K. A. Abboud and G. Christou, *Angew. Chem. Int. Ed.*, 2004, **43**, 345-349; (c) A. W. Coleman, D. F. Jones, P. H. Dixneuf, C. Brisson, J.-J. Bonnet and G. Lavigne, *Inorg. Chem.,* 1984, **23**, 952-956.

11 (a) F. He, M.-L. Tong and X.-M. Chen, *Inorg. Chem.*, 2005, **44(23)**, 8285-8292; (b) Y. Sadaoka, E. Traversa and M. Sakamoto*, J. Mater. Chem*., 1996, **6**, 1355-1360; (c) M. C. Carotta, G. Martinelli, Y. Sadaoka, P. Nunziante and E. Traversa, *Sens. Actuators, B,* 1998, **48**, 270-276

12 (a) A. Jana, B. J. Crowston, J. R. Shewring, L. K. McKenzie, H. E. Bryant, S. W. Botchway, A. D. Ward, A. J. Amoroso, E. Baggaley and M. D. Ward, *Inorg. Chem*., 2016, **55**, 5623-5633; (b) S. Realista, P. Ramgi, B. de P. Cardoso, A. I. Melato, A. S. Viana, M. J. Calhorda and P. N. Martinho, *Dalton Trans*., 2016, **45**, 14725-14733; (c) M. I. Szávuly, M. Surducan, E. Nagy, M. Surányi, G. Speier, R. Silaghi-Dumitrescu and J. Kaizer, *Dalton Trans*., 2016, **45**, 14709-14718.

13 (a) N. V. Sidgwick and H. M. Powell, *Proc. R. Soc. (London),* 1940, **A176**, 153; (b) D. R. McKeney, *J. Chem. Educ.,* 1983, **60**, 112-116; (c) M. S. Banna, *J. Chem. Educ.,* 1985, **62**, 197-198; (d) K. S. Pitzer, *Acc. Chem. Res*., 1979, **12**, 271-276; (e) P. Pyykko¨, J.-P. Desclaux, *Acc. Chem. Res*., 1979, **12**, 276-281; (f) P. Pyykko¨, *Chem. Rev.,* 1988, **88**, 563-594.

14 (a) D. L. Reger, M. F. Huff, A. L. Rheingold and B. S. Haggert, *J. Am. Chem. Soc*., 1992, **114**, 579-584; (b) R. J. Gillespie and R. S. Nyholm, *Q. Rev. London*, 1957, **11**, 339-380; (c) R. J. Gillespie and I. Hargittai, *The VESPR Model of Molecular Geometry*; Allyn and Bacon: Boston, MA, 1991.

View Article Online
DOI: 10.1039/C7NJ05148D

15 (a) R. D. Hancock, J. H. Reibenspies and H. Maumela, *Inorg. Chem*., 2004, **43**, 2981-2987; (b) R. Luckay, I. Cukrowski, J. Mashishi, J. H. Reibenspies, A. H. Bond, R. D. Rogers and R. D. Hancock, *J. Chem. Soc., Dalton Trans*., 1997, 901-908; (c) A. Walsh and G. W. Watson, *J. Solid State Chem*., 2005, **178**, 1422-1428; (d) R. D. Hancock, M. S. Shaikjee, S. M. Dobson and J. C. Boeyens, *Inorg. Chim. Acta,* 1988, **154**, 229-238; (e) D. Esteban-Gómez, C. Platas-Iglesias, T. Enrıquez-Pérez, F. Avecilla, A. Blas and T. Rodrıguez-Blas, *Inorg. Chem*., 2006, **45**, 5407-5416; (f) C. Platas-Iglesias, D. Esteban-Gomez, T. Enriquez-Perez, F. Avecilla, A. D. Blas and T. Rodriguez-Blas, *Inorg. Chem*., 2005, **44**, 2224-2233.

16 (a) P. Politzer, J. S. Murray and T. Clark, *Phys. Chem. Chem. Phys.*, 2013, **15**, 11178-11189; (b) A. Bauzá, T. J. Mooibroek and A. Frontera, *ChemPhysChem*, 2015, **16**, 2496-2517; (c) A. Bauzá and A. Frontera, *Angew. Chem. Int. Ed.*, 2015, **54**, 7340-7343.

17 (a) J. S. Murray, K. E. Riley, P. Politzer and T. Clark, *Aust. J. Chem*., 2010, **63**, 1598-1607; (b) P. Politzer and J. S. Murray, *ChemPhysChem*, 2013, **14**, 278-294; (c) P. Politzer, J. S. Murray and T. Clark, *Phys. Chem. Chem. Phys.*, 2010, **12**, 7748-7757; (d) P. Politzer, K. E. Riley, F. A. Bulat and J. S. Murray, *Comput. Theor. Chem.*, 2012, **998**, 2-8; (e) A. Bauzá, I. Alkorta, A. Frontera and J. Elguero, *J. Chem. Theory Comput*., 2013, **9**, 5201-5210; (f) G. Sánchez-Sanz, C. Trujillo, I. Alkorta and J. Elguero, *Phys. Chem. Chem. Phys*., 2014, **16**, 15900-15909.

18 (a) A. Bauzá, T. J. Mooibroek and A. Frontera, *Angew. Chem. Int. Ed.*, 2013, **52**, 12317-12321; (b) S. J. Grabowski, *Phys. Chem. Chem. Phys.*, 2014, **16**, 1824-1834; (c) A. Bauzá, T. J. Mooibroek and A. Frontera, *Chem. -Eur. J*., 2014, **20**, 10245-10248; (d) E. C. Escudero-Adán, A. Bauzá, A. Frontera and P. Ballester, *ChemPhysChem*, 2015, **16**, 2530-2533; (e) A. Bauzá, T. J. Mooibroek

View Article Online
DOI: 10.1039/C7NJ05148D

and A. Frontera, *Phys. Chem. Chem. Phys*., 2014, **16**, 19192-19197; (f) A. Bauzá, T. J. Mooibroek and A. Frontera, *Chem. Commun*., 2014, **50**, 12626-12629; (g) A. Bauzá, T. J. Mooibroek and A. Frontera, *Chem. Rec*., 2016, **16**, 473-487; (h) J. S. Murray, P. Lane and P. Politzer, *J. Mol. Model*, 2009, **15**, 723-729; (i) A. Bundhun, P. Ramasami, J. S. Murray and P. Politzer, *J. Mol. Model*, 2013, **19**, 2739-2746; (j) R. S. Ruoff, T. Emilsson, A. I. Jaman, T. C. Germann and H. S. Gutowsky, *J. Chem. Phys.*, 1992, **96**, 3441-3446; (k) R. -D. Urban, G. Rouillé and M. Takami, *J. Mol. Struct.*, 1997, **413**-**414**, 511-519; (l) I. Alkorta, I. Rozas and J. Elguero, *J. Phys. Chem. A,* 2001, **105**, 743-749.

19 M. Servati Gargari, V. Stilinović, A. Bauzá, A. Frontera, P. McArdle, D. Van Derveer, S. W. Ng and G. Mahmoudi, *Chem. -Eur. J*., 2015, **21**, 17951-17958.

20 G. Mahmoudi, A. Bauzá and A. Frontera, *Dalton Trans*., 2016, **45**, 4965-4969.

21 (a) C. Gourlaouen, O. Parisel and H. Gerard, *Dalton Trans.,* 2011, **40**, 11282-11288; (b) L. Shimoni-Livny, J. P. Glusker and C. W. Bock, *Inorg. Chem.*, 1998, **37**, 1853-1867; (c) R. L. Davidovich, V. Stavila, D. V. Marinin, E. I. Voit and K. H. Whitmire, *Coord. Chem. Rev*., 2009, **253**, 1316-1352.

22 K. P. Sharma, and R. K. Poddar, *Transition Met. Chem*., 1984, **9**, 135-138.

23 CRYSALIS, v1, Oxford Diffraction Ltd., Oxford, UK, 2005.

24 G. M. Sheldrick, SHELXS-97 and SHELXL-97, Program for Structure Solution, University of Gottingen, Germany, 1997.

View Article Online
DOI: 10.1039/C7NJ05148D

25 A. L. Spek, *Acta Crystallogr., Sect. A: Cryst. Phys., Diffr., Theor. Gen. Crystallogr.*, 1990, **46**, C34.

26 K. Diamond, Crystal Impact GbR, Germany, Bonn, 2007.

27 M. N. Burnett and C. K. Johnson, ORTEP-3: Oak Ridge Thermal Ellipsoid Plot Program for Crystal Structure Illustrations, Report ORNL-6895, Oak Ridge National Laboratory, Oak Ridge, TN, USA, 1996.

28 C. F. Macrae, I. J. Bruno, J. A. Chisholm, P. R. Edgington, P. McCabe, E. Pidcock, L. R. Monge, R. Taylor, J. van de Streek and P. A. Wood, *J. Appl. Crystallogr.*, 2008, **41**, 466-470.

29 (a) M. A. Spackman and D. Jayatilaka, *CrystEngComm*, 2009, **11**, 19-32; (b) F. L. Hirshfeld, *Theor. Chim. Acta*, 1977, **44**, 129-138; (c) H. F. Clausen, M. S. Chevallier, M. A. Spackman and B. B. Iversen, *New J. Chem.*, 2010, **34**, 193-199.

30 S. K. Wolff, D. J. Grimwood, J. J. McKinnon, D. Jayatilaka and M. A. Spackman, *Crystal Explorer 2.0*, University of Western Australia, Perth, Australia, 2007, http:// hirshfeldsurfacenet.blogspot.com.

31 R. Ahlrichs, M. Bär, M. Häser, H. Horn and C. Kölmel, *Chem. Phys. Lett.*, 1989, **162**, 165-169.

32 S. F. Boys and F. Bernardi, *Mol. Phys.*, 1970, **19**, 553-566.

33 R. F. W. Bader, *Chem. Rev.*, 1991, **91**, 893-928.

34 T. A. Keith, AIMAll (Version 13.05.06), TK Gristmill Software, Overland Park KS, USA, 2013.

35 (a) P. Bhowmik, S. Jana, P. P. Jana, K. Harms and S. Chattopadhyay, *Inorg. Chim. Acta*, 2012, **390**, 53-60. (b) S. Bhattacharya and S. Mohanta, *Inorg. Chim. Acta*, 2015, **432**, 169-175; (c) A. Jana and S. Mohanta, *CrystEngComm*, 2014, **16**, 5494-5515.

View Article Online
DOI: 10.1039/C7NJ05148D

36 (a) S. Bhattacharya, A. Jana and S. Mohanta, *CrystEngComm*, 2013, **15**, 10374-10382; (b) L. Salmon, P. Thu´ery and M. Ephritikhine, *Dalton Trans*., 2004, 4139-4145.

37 (a) J. H. Thurston, C. G.-Z. Tang, D. W. Trahan and K. H. Whitmire, *Inorg. Chem.,* **2004**, *43*, 2708-2713; (b) S. Bhattacharya and S. Mohanta, *Inorg. Chim. Acta,* **2015**, 432, 169-175; (c) A. Mustapha, K. Busch, M. Patykiewicz, A. Apedaile, J. Reglinski, A. R. Kennedy and T. J. Prior, *Polyhedron*, **2008**, *27*, 868-878; (d) J. Reglinski, S. Morris and D. E. Stevenson, *Polyhedron*, **2002**, *21*, 2167-2174; (e) S. Sarkar and S. Mohanta, *RSC Adv.,* **2011***, 1,* 640-650; (f) K. Inoue, M. Ohba and H. Ōkawa, *Bull. Chem. Soc. Jpn.,* **2002***, 75,* 99-107.

38 (a) S. Roy, A. Bhattacharyya, S. Purkait, A. Bauza, A. Frontera and S. Chattopadhyay, *Dalton Trans*., 2016, **45**, 15048-15059; (b) S. Roy, Michael G. B. Drew, A. Bauza, A. Frontera and S. Chattopadhyay, *ChemistrySelect*, 2017, **2**, 7880-7887; (c) S. Roy, Michael G. B. Drew, A. Bauza, A. Frontera and S. Chattopadhyay, *ChemistrySelect*, 2017, **2**, 10586-10594.

39 (a) R. Kurtaran, L. T. Yildirim, A. D. Azaz, H. Namli, O. Atakol, *J. Inorg. Biochem*., 2005, **99**, 1937-1944; (b) S. Hazra, S. Sasmal, M. Nayak, H. A. Sparkes, J. A. K. Howard and S. Mohanta, *CrystEngComm*, 2010, **12**, 470-477; (c) S. Mondal, S. Hazra, S. Sarkar, S. Sasmal and S. Mohanta, *J. Mol. Struct*., 2011, **1004**, 204-214; (d) Edwin C. Constable, G. Zhang, C. E. Housecroft, M. Neuburger, J. A. Zampese, *Inorg. Chim. Acta*, 2010, **363**, 4207-4213.

40 (a) A. Bhattacharyya, S. Roy, J. Chakraborty and S. Chattopadhyay, *Polyhedron*, 2016, **112**, 109-117; (b) P. Bhowmik, H. P. Nayek, M. Corbella, N. Aliaga-Alcalde, S. Chattopadhyay, *Dalton Trans*., 2011, **40**, 7916-7926.

View Article Online
DOI: 10.1039/C7NJ05148D

41 (a) A. Bhattacharyya, K. Harms and S. Chattopadhyay, *Inorg. Chem. Commun*., 2014, **48**, 12-17; (b) 28 Z. -L. You, D. -M. Xian and M. Zhang, *CrystEngComm*, 2012, **14**, 7133-7136; (c) S. Roy, A. Dey, P. P. Ray, J. Ortega-Castro, A. Frontera and S. Chattopadhyay, *Chem. Commun*., 2015, **51**, 12974-12976.

42 (a) K. Nakamoto, *Infrared and Raman Spectra of Organic and Coordination Compounds*, John Wiley and Sons, New York, 3rd edn, 1978, p. 227; (b) P. Bhowmik, K. Harms and S. Chattopadhyay, *Polyhedron*, 2013, **49**, 113-120.

43 (a) K. Nakamoto, *Infrared and Raman Spectra of Organic and Coordination Compounds*, John Wiley and Sons, New York, 3rd edn, 1978, p. 235-236; (b) S. Chattopadhyay, M. G. B. Drew and A. Ghosh, *Eur. J. Inorg. Chem.,* 2008, 1693-1701.

44 (a) A. Bhattacharyya, P. K. Bhaumik, M. Das, A. Bauzá, P. P. Jana, K. Harms, A. Frontera and S. Chattopadhyay, *Polyhedron*, 2015, **101**, 257-269; (b) S. Chattopadhyay, M. G. B. Drew and A. Ghosh, *Polyhedron*, 2007, **26**, 3513-3522.

45 (a) S. Roy, M. G. B. Drew, A. Bauzá, A. Frontera and S. Chattopadhyay, *Dalton Trans*., 2017, **46**, 5384-5397; (b) M. Nazarov and D. Y. Noh, *New Generation of Europium- and Terbium-Activated Phosphors: From Syntheses to applications*, Pan Stanford Publishing, 6000 Broken Sound Pkwy NW, 2011, p. 211.

46 J. Costamagna, J. Vargas, R. Latorre, A. Alvarado and G. Mena, *Coord. Chem. Rev*., 1992, **119**, 67-88.

View Article Online
DOI: 10.1039/C7NJ05148D

47 A. Bhattacharyya, P. K. Bhaumik, P. P. Jana and S. Chattopadhyay, *Polyhedron*, 2014, **78**, 40-45.

48 (a) A. Bauzá and A. Frontera, *ChemPhysChem*, 2015, **16**, 3108-3113; (b) A. Bauzá and A. Frontera, *ChemPhysChem*, 2015, **16**, 3625-3630; (c) M. Mirzaei, M. Nikpour, A. Bauza and A. Frontera, *ChemPhysChem*, 2015, **16**, 2260-2266; (d) A. Bauzá and A. Frontera, *Chem. Phys. Lett.*, 2015, **633**, 282-286.

View Article Online
DOI: 10.1039/C7NJ05148D

Non-covalent tetrel bonding interactions in hemidirectional lead(II) complexes with nickel(II)-salen type metalloligands

Sourav Roy, Michael G. B. Drew, Antonio Bauzá, Antonio Frontera and Shouvik Chattopadhyay

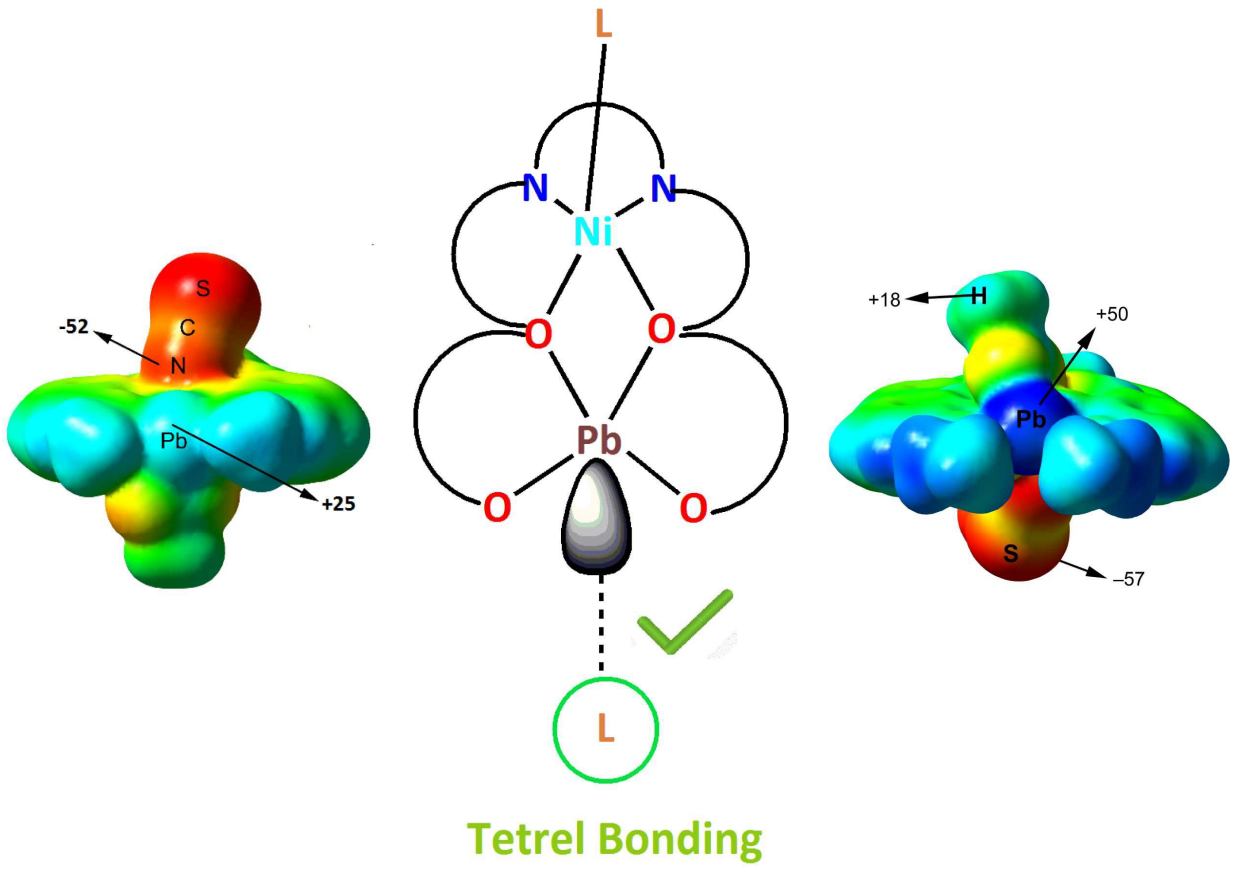

Tetrel bonding interactions have been investigated in hetero-dinuclear nickel(II)/lead(II) complexes by MEP and DFT calculations.